

CHAPTER ONE

INTRODUCTION

1.1 Motivation

Recently, the studies of Variable Structure Control (VSC) of nonlinear systems have attracted lots of attention. It is known that the VSC scheme has many advantages, such as fast response, small sensitivity to system uncertainties and disturbances from the environment, easily designed and so on, which is better than other methods used before [30], [35]. Base on these reasons, the VSC approach has been popularly put in use to a variety of control issues [8], [36], and one of those applications is spacecraft attitude control issue. Nevertheless, among the existing publications, almost all the relative researches about VSC control problem adopted either conventional sign-type or saturation-type schemes to obtain the VSC controller to make the system states to reach some specified sliding surfaces. Generally speaking, the conventional VSC schemes maybe can reach the demand tasks, however, both of them have their won drawbacks. For example, the sign-type VSC scheme usually result in high frequency chattering behavior due to the discontinuous switching control law. The influence of chattering behavior includes undesired excitation of unmodeled dynamics of the system, waste of energy when the system states are around the sliding surface [30], and the most seriously, to damage the mechanisms of the system. Similarly, although the saturation-type VSC design one with fixed boundary layer width can decrease the high frequency behavior as a result of sign-type VSC method, it can only achieve uniformly ultimate boundedness performance [2]. To overcome the shortcomings, this thesis utilizes the VSC design technique to synthesize a class of continuous control laws. The modified control laws are able to alleviate chattering behavior of the sign-type VSC scheme and also promote the performance of the saturation-type VSC one from a

level uniformly ultimate boundedness to asymptotic stability. To interpret the excellence of the proposed schemes, we will demonstrate the simulation results of spacecraft attitude stabilization issue, which will verify the theorem we suggest. Furthermore, since the VSC design is now a very popular and well known control technique, the concept and the detail design process will not be mentioned in this thesis again, we treat it as a pre-knowledge here.

On the other hand, as a result of the fast growing demands of system reliability in aerospace and industrial process, the research of reliable control is a popular issue in recent years. Such as the spacecraft, once it suffers outage on the orbit, the reparation is an expensive and time wasting task, and can not be achieved immediately. Therefore, the object of reliable control is to design an appropriate controller such that the closed-loop system can tolerate the abnormal operation of some specific control components for the purpose to maintain an overall system stability and acceptable performance of the system. An abnormal operation may include amplification, degradation, or most seriously, uncontrollable. Among the present reliable control schemes, many approaches have been proposed, for example, HJ-based approach [16], [37] or power series method [12]. The HJ-based approach is mainly for nonlinear systems, an inevitable difficulty comes from its controller design depend upon the solutions of the Hamilton-Jacobi equation or inequality, which are known with troubling computation procedure and hard to solve, but is an necessary part of the design of LQR and H-infinity controllers. On the other hand, although the power series method can relax the difficulty of the HJ-based approach, unfortunately, the obtained solutions are only approximated ones, and the calculation loading may grow very fast when the system becomes complicated. Summarizing these potential drawbacks, this thesis progresses the reliable issues from VSC viewpoint. Here, we propose a class of reliable VSC control laws, which are easily implemented and do not need the solutions of a Hamilton-Jacobi equation or inequality, and we will shown that these schemes are be able to tolerate the outage of actuators within some prespecified subset.

In general, the designs of reliable control system [?] can be classified as passive ones

[13], [15], [16] and active ones [1], [19], [25]. In an passive reliable control, the system exploits inherent redundancy to design a fixed controller so that the closed-loop system can achieve an acceptable performance not only during normal operation but also under the situations that various components fail. The defect of passive control is the pre-specified fault condition must be selected, if the practical outage is not within the range as we expected, the passive scheme may fail. On the contrary, the active approach utilize a fault detection and diagnosis (FDD) scheme to identify the faults, and the controller will be reconfigured according to the on-line detection results in real time. The drawback of active scheme is mainly come from FDD, including its stability, external noise resist ability, the threshold of alarms and so on, while these will not necessary to be considered when a passive controller is used. In this thesis, both passive and active reliable control designs will be considered.

Finally, we finish the thesis with discussing an important issue of a control system: *controllability*. Although there are many and simple methods to determine the controllability of a system, the existing methods to test the controllability involve determining whether or not a certain matrix has rank equal to the order of the system. However, these tests provide only "yes" or "not" answer for the controllability of a system, generally speaking, do not provide satisfactory one due to the finite accuracy of the computation and the parameters of a system ,which are known only approximately. Base on these reasons, we will introduce two new viewpoints for controllability, which are continuous measurements. The first one is "The Distance to Uncontrollable" (see e.g., [3], [10], [7], [11], [24], [26]), the concept of it is to define an uncontrollable set, then find out the shortest distance form the original system to it. The inconvenient of this method is one must to determine the singular value of a polynomial matrix and minimizing a function of a complex variable, which is complicated. The second one is "Mobility of Eigenvalues", proposed by Tarokh [31], [33], [34], the point of view of this manner is to determine the ability of an eigenvalue to move a very small distance to the neighborhood of its own. Both two methods have their own opinions and benefits, and we will give detailed interpretations in this thesis.

1.2 Outline

This thesis is organized as follows. Chapter 2 proposes a reliable controller design for nonlinear system using VSC design technique and its applications to spacecraft, and the associated simulations. Chapter 3 gives detailed interpretations about the two new controllability measurements, "The Distance to Uncontrollable" and "Mobility of Eigenvalues". Finally, in chapter 4, we give the conclusions and suggestions for the researches in the future.



CHAPTER TWO

RELIABLE VARIABLE STRUCTURE CONTROL OF NONLINEAR SYSTEMS

2.1 Introduction

Due to the growing demands of system reliability in aerospace and industrial process, the research of reliable control [17], [18], [19], [20], [21], [22], [23] is a popular issue in recent years. The object of this chapter is to design an appropriate reliable controller such that the closed-loop system can tolerate the abnormal operation of some specific control components for the purpose to maintain an overall system stability and acceptable system performance. An abnormal operation may include amplification, degradation partial fail, or most seriously, uncontrollable. In general, the designs of reliable control system can be classified as passive one [13], [15], [16] and active one [1], [19], [25], and both of them will be proposed in this chapter. The active approach utilizes a fault detection and diagnosis (FDD) scheme to identify the faults, and the controller will be reconfigured according to the on-line detection results in real time, while the passive control must pre-specify the fault condition, and exploit inherent redundancy to design a fixed controller so that the closed-loop system stability can be achieved not only during normal operation but also when some of the actuators experience faults.

Besides, the studies of Variable Structure Control (VSC) of nonlinear systems have attracted lots of attention. It is known that the VSC scheme have many advantages, like fast response, small sensitivity to system uncertainties and disturbance form the environment, easily designed and so on, which is better than other methods used before [30], [35]. Base on these reasons, the VSC approach has been popularly applied to a variety of control issues [8], [36] and one of those applications is spacecraft attitude control.

In this chapter, we will propose a reliable control scheme for nonlinear system via variable structure control technique and give the applications to a spacecraft in the last.

2.2 Reliable Stabilization Control Design via VSC Scheme

2.2.1 Problem Formulation

Consider a set of second-order nonlinear system as described by

$$\dot{\mathbf{x}}_1 = \mathbf{x}_2 \quad (2.1)$$

$$\dot{\mathbf{x}}_2 = \mathbf{f}(\mathbf{x}) + G(\mathbf{x})\mathbf{u} + \mathbf{d} \quad (2.2)$$

where $\mathbf{x} = (\mathbf{x}_1^T, \mathbf{x}_2^T)^T \in \mathbb{R}^{2n}$, $\mathbf{u} \in \mathbb{R}^{n+m}$ and $\mathbf{d} \in \mathbb{R}^n$ denote the system states, control inputs, and possible model uncertainties or external disturbances, respectively, and $\mathbf{f}(\mathbf{x}) \in \mathbb{R}^n$ and $G(\mathbf{x}) \in \mathbb{R}^{n \times (n+m)}$ are assumed to be smooth. More precisely, the denotations above are $\mathbf{x}_1 := (x_1, \dots, x_n)^T \in \mathbb{R}^n$, $\mathbf{x}_2 := (x_{n+1}, \dots, x_{2n})^T \in \mathbb{R}^n$, $\mathbf{u} := (u_1, \dots, u_{n+m})^T$, and $\mathbf{d} := (d_1, \dots, d_n)^T$, while $(\cdot)^T$ denote the transpose of a vector or a matrix. In addition, for the interest of study, we assume that $\mathbf{f}(\mathbf{0}) = \mathbf{0}$. Also note that, as shown in system (2.1)-(2.2), we have assume that the system with inherent control input redundancy.

The objective of this section is to synthesize a control law that under which the stabilization task can be achieved even when the control experiences actuator outage with the number of remainder healthy actuators being no less than n . Here, we will propose both passive and active reliable designs. In passive ones, the system exploits inherent redundancy to design a fixed controller so that the closed-loop system can achieve an acceptable performance not only during normal operation but also under various faults, while the active ones reconfigure the control laws according to the on-line detection results after the occurrence of faults. For this reason, the active reliable controls need the information of FDD scheme while those of passive ones do not. In the following, both passive and active reliable schemes will be established by the use of the VSC design technique.

2.2.2 Passive Reliable Design

To begin with, we pre-divide the actuators into two groups \mathcal{F} and \mathcal{H} , for the purpose to endure the faults, we assume that the faulty actuators in group \mathcal{F} must be tolerated,

while the ones in group \mathcal{H} are healthy during the operation. The system (2.1)-(2.2) can be rewritten as

$$\dot{\mathbf{x}}_1 = \mathbf{x}_2 \quad (2.3)$$

$$\dot{\mathbf{x}}_2 = \mathbf{f}(\mathbf{x}) + G_{\mathcal{H}}(\mathbf{x})\mathbf{u}_{\mathcal{H}} + G_{\mathcal{F}}(\mathbf{x})\mathbf{u}_{\mathcal{F}} + \mathbf{d} \quad (2.4)$$

Since the nonsingularity assumption of $G_{\mathcal{H}}(\mathbf{x})$ is necessary for the existence of equivalent control in VSC design when all the actuators in \mathcal{F} fail to operate, we assume that the pre-specified healthy actuators in \mathcal{H} satisfy $\mathbf{u}_{\mathcal{H}} \in \mathbb{R}^n$ and $G_{\mathcal{H}}(\mathbf{x}) \in \mathbb{R}^{n \times n}$ is a nonsingular matrix, while the faulty ones in \mathcal{F} satisfy $\mathbf{u}_{\mathcal{F}} \in \mathbb{R}^m$ and $G_{\mathcal{F}}(\mathbf{x}) \in \mathbb{R}^{n \times m}$. Although the number of remainder healthy actuators may greater than n , base on the reason that the fewer healthy actuators we need to stabilize the control system, the more actuators are allowed to be fail, which the more faulty conditions the system can be. Therefore, the assumption implies that the pre-selected susceptible actuators have assumed to be as many as possible.

All Actuators in F are Fail

Now, we first consider the design of $\mathbf{u}_{\mathcal{H}}$ when all the actuators in \mathcal{F} work abnormally, and define $\mathbf{u}_{\mathcal{F}}^*$ and $\mathbf{u}_{\mathcal{F}}$ denote the actual and the designed control values for those actuators in \mathcal{F} , respectively, and the system (2.3)-(2.4) becomes

$$\dot{\mathbf{x}}_1 = \mathbf{x}_2 \quad (2.5)$$

$$\begin{aligned} \dot{\mathbf{x}}_2 &= \mathbf{f}(\mathbf{x}) + G_{\mathcal{H}}(\mathbf{x})\mathbf{u}_{\mathcal{H}} + G_{\mathcal{F}}(\mathbf{x})\mathbf{u}_{\mathcal{F}}^* + \mathbf{d} \\ &= \mathbf{f}(\mathbf{x}) + G(\mathbf{x})\mathbf{u} + G_{\mathcal{F}}(\mathbf{x})(\mathbf{u}_{\mathcal{F}}^* - \mathbf{u}_{\mathcal{F}}) + \mathbf{d} \end{aligned} \quad (2.6)$$

The idea of approach here is to treat the fault term $G_{\mathcal{F}}(\mathbf{x})(\mathbf{u}_{\mathcal{F}}^* - \mathbf{u}_{\mathcal{F}})$ as an additional disturbance and establish a control law to compensate it.

It is known that the VSC design consists of following procedures:

Step 1: To choose an appropriate sliding surface in terms of states.

Step 2: To synthesize a control law in the form of

$$\mathbf{u} = \mathbf{u}^{re} + \mathbf{u}^{eq} \quad (2.7)$$

to achieve the tracking performance, where their roles are

\mathbf{u}^{re} : Making the states reach the sliding surface in a finite time.

\mathbf{u}^{eq} : Keeping the sliding surface an invariant set and directs the states to the origin.

According to these procedures, we now begin to design the control law. Following step 1, choose a sliding surface as

$$\mathbf{s} = \mathbf{x}_2 + M\mathbf{x}_1 = \mathbf{0} \quad (2.8)$$

where $\mathbf{s} := (s_1, \dots, s_n)^T \in \mathbb{R}^n$ is the sliding vector, and $M \in \mathbb{R}^{n \times n}$ is a positive-definite matrix. It is noted that once the system states keep staying on the sliding surface, then the system will enter *sliding mode*, then utilizes the fact that $\mathbf{x}_2 = \dot{\mathbf{x}}_1$, the reduced model will have the form

$$\mathbf{s} = \dot{\mathbf{x}}_1 + M\mathbf{x}_1 = \mathbf{0} \quad (2.9)$$

We have known that efficiency of input term \mathbf{u}^{re} is to make the states reach the sliding surface in a finite time, that is, the sliding surface \mathbf{s} will converge to zero in a finite time, then equation (2.9) can be held and \mathbf{x}_1 will approach to $\mathbf{0}$ exponentially. Note that since $\mathbf{x}_2 = \dot{\mathbf{x}}_1 = -M\mathbf{x}_1$, the state \mathbf{x}_2 will also close to $\mathbf{0}$ exponentially, then the stabilization performance will be fulfilled and the main goal of the control is achieved. Furthermore, if the specified matrix M is more positive, then the faster the speed of convergence of the system states will be. Now, according to step 2, we design \mathbf{u}^{eq} first. From equations (2.5)-(2.6) and (2.8) we can have

$$\begin{aligned} \dot{\mathbf{s}} &= \dot{\mathbf{x}}_2 + M\dot{\mathbf{x}}_1 \\ &= \mathbf{f}(\mathbf{x}) + G_{\mathcal{H}}(\mathbf{x})\mathbf{u}_{\mathcal{H}} + G_{\mathcal{F}}(\mathbf{x})\mathbf{u}_{\mathcal{F}}^* + \mathbf{d} + M\mathbf{x}_2 \end{aligned} \quad (2.10)$$

here, we treat the unknown terms $G_{\mathcal{F}}(\mathbf{x})\mathbf{u}_{\mathcal{F}}^*$ and \mathbf{d} as disturbances, ignore them and let $\dot{\mathbf{s}} = 0$ thus we can get the equivalent control

$$\mathbf{u}^{eq} = -G_{\mathcal{H}}^{-1}(\mathbf{x})\{\mathbf{f}(\mathbf{x}) + M\mathbf{x}_2\} \quad (2.11)$$

When design \mathbf{u}^{re} , in order to compensate the effect of disturbances and faults, we impose the next assumption, in which $(\cdot)_i$ denotes the i -th element of a vector.

Assumption 2.1 There exist nonnegative scalar functions $\rho_i(\mathbf{x}, t)$ such that, for $i = 1, \dots, n$,

$$|(G_{\mathcal{F}}(\mathbf{x})\mathbf{u}_{\mathcal{F}}^*)_i| + |d_i| \leq \rho_i(\mathbf{x}, t) \quad (2.12)$$

■

Following the VSC design procedure, we can let the reach control as

$$\mathbf{u}^{re} = -G_{\mathcal{H}}^{-1}(\mathbf{x})\{\Lambda_{\mathcal{H}} \cdot \text{sgn}(\mathbf{s})\} \quad (2.13)$$

where $\Lambda_{\mathcal{H}} = \text{diag}(\rho_1(\mathbf{x}, t) + \eta_1, \dots, \rho_n(\mathbf{x}, t) + \eta_n)$ with $\eta_i > 0$ for all $i = 1, \dots, n$, and $\text{sgn}(\cdot)$ denotes the sign function and $\text{sgn}(\mathbf{s}) := (\text{sgn}(s_1), \dots, \text{sgn}(s_n))^T$.

Integrating \mathbf{u}^{eq} and \mathbf{u}^{re} together, we can get the overall control torque

$$\begin{aligned} \mathbf{u}_{\mathcal{H}} &= \mathbf{u}^{eq} + \mathbf{u}^{re} \\ &= -G_{\mathcal{H}}^{-1}(\mathbf{x})\{\mathbf{f}(\mathbf{x}) + M\mathbf{x}_2 + \Lambda_{\mathcal{H}} \cdot \text{sgn}(\mathbf{s})\} \end{aligned} \quad (2.14)$$

in order to show the stabilization of the system, we define the squared "distance" to the sliding surface, as measured by $\|\mathbf{s}\|^2$, where $\|\cdot\|$ denotes the Euclidean norm, then the variation of the distance with respect to t can be expressed as

$$\frac{1}{2} \frac{d}{dt} \|\mathbf{s}\|^2 = \mathbf{s}^T \dot{\mathbf{s}} \quad (2.15)$$

under such a control, it follows from equations (2.10), (2.14) and Assumption 2.1 that

$$\begin{aligned} \mathbf{s}^T \dot{\mathbf{s}} &= \mathbf{s}^T \{\mathbf{f}(\mathbf{x}) + G_{\mathcal{H}}(\mathbf{x})(\mathbf{u}^{eq} + \mathbf{u}^{re}) + G_{\mathcal{F}}(\mathbf{x})\mathbf{u}_{\mathcal{F}}^* + \mathbf{d} + M\mathbf{x}_2\} \\ &= \mathbf{s}^T \{G_{\mathcal{F}}(\mathbf{x})\mathbf{u}_{\mathcal{F}}^* + \mathbf{d} - \Lambda_{\mathcal{H}} \cdot \text{sgn}(\mathbf{s})\} \\ &\leq -\sum_{i=1}^n \eta_i \cdot |s_i| \end{aligned} \quad (2.16)$$

this inequality implies the distance decreases along all the system states, it constrains the system states to point toward the sliding surface in a finite time, besides, the larger the constants η_1, \dots, η_n we select, the faster the first time the system states reach the sliding surface.

Not All Actuators in \mathcal{F} are Fail

In addition to the design of $\mathbf{u}_{\mathcal{H}}$ as discussed above, we now investigate the design of $\mathbf{u}_{\mathcal{F}}$ to promote the system performance when not all the actuators in \mathcal{F} are fail. The

governing equations are now given by (2.3)-(2.4). From equations (2.3)-(2.4), (2.8) and (2.14) we can obtain

$$\begin{aligned} \mathbf{s}^T \dot{\mathbf{s}} &= \mathbf{s}^T \{ \mathbf{f}(\mathbf{x}) + G_{\mathcal{H}}(\mathbf{x})\mathbf{u}_{\mathcal{H}} + G_{\mathcal{F}}(\mathbf{x})\mathbf{u}_{\mathcal{F}} + \mathbf{d} + M\mathbf{x}_2 \} \\ &\leq \mathbf{s}^T G_{\mathcal{F}}(\mathbf{x})\mathbf{u}_{\mathcal{F}} - \sum_{i=1}^n \eta_i \cdot |s_i| \end{aligned} \quad (2.17)$$

and one of the choices of $\mathbf{u}_{\mathcal{F}}$ to make the system states to approach the sliding surface faster than the case which $\mathbf{u}_{\mathcal{F}} = \mathbf{0}$ is

$$\mathbf{u}_{\mathcal{F}} = -\Lambda_{\mathcal{F}} \cdot \text{sgn}(G_{\mathcal{F}}^T(\mathbf{x})\mathbf{s}) \quad (2.18)$$

where $\Lambda_{\mathcal{F}} = \text{diag}(\eta_{n+1}, \dots, \eta_{n+m})$ and η_{n+i} , for $i = 1, \dots, m$ are some positive constants. Adding the control $\mathbf{u}_{\mathcal{F}}$ as shown in equation (2.18) into the system, the equation (2.17) becomes

$$\mathbf{s}^T \dot{\mathbf{s}} \leq - \sum_{i=1}^n \eta_i \cdot |s_j| - \sum_{i=n+1}^{n+m} \eta_i \cdot |(G_{\mathcal{F}}(\mathbf{x})^T \mathbf{s})_i| \quad (2.19)$$

It can be seen from the derivation that the magnitude of control gains η_{n+i} , $i = 1, \dots, m$, of actuators in $\mathbf{u}_{\mathcal{F}}$ can be vary from $\mathbf{0}$ to the allowable maximum control input magnitude to accelerate the speed of the system states to sliding surface. That is, the situation of actuators in \mathcal{F} can be total failure, partial failure, attenuation or amplification, no matter in any order and any combination. These derivations lead to the following result.

Theorem 2.1 Suppose the Assumption 2.1 holds, then the origin of system (2.3)-(2.4) is locally asymptotically stable under the control laws given by (2.14) and (2.18), even some or all the actuators in \mathcal{F} experience abnormal operation. ■

2.2.3 Active Reliable Design

The reliable design discussed above is the passive one which does not need the information of FDD, but does need to pre-specify which actuators are allowed to fail. It should be noted that, it is very difficult to define the healthy and the fault actuators before faults occur, in general. Although the passive reliable control might achieve stabilization performance, it is a conservative method in that its controllers are designed based on the pre-defined faulty system without any change in control law even when faults occur. Due

to the lack of FDD information, the passive reliable design often overestimates the magnitude of faults, that is, the magnitude of $(G_{\mathcal{F}}(\mathbf{x})\mathbf{u}_{\mathcal{F}}^*)_i$, for $i = 1, \dots, n$, where is shown in Assumption 2.1. Although the overestimation can speed up the convergence to the sliding surface, but usually result in undesirable performance, such as wasting of control energy and causing the designed control to exceed the allowable maximum control input magnitude. To improve the performance of passive reliable control, we consider the active control issue in this section.

During the normal operation, the engineers may take any desired control to fulfill the system performance. When faults happened, the control law will be switched to an active reliable control type, as described below. Without loss of generality, we assume the faults happen at control channels

$$\{u_{k+1}, \dots, u_{n+m}\}, \quad k \geq n \quad (2.20)$$

and the actual control torque of the faulty control channels are successfully detected and diagnosed as

$$u_j^* = \hat{u}_j + \Delta u_j \quad (2.21)$$

where $j = k+1, \dots, n+m$, and $\hat{u}_j, \Delta u_j$ denote the estimated control value and estimated error, respectively. With the same definition of the sliding surface in equation (2.8) and system (2.1)-(2.2) we can have

$$\begin{aligned} \dot{\mathbf{s}} &= \dot{\mathbf{x}}_2 + M\dot{\mathbf{x}}_1 \\ &= \mathbf{f}(\mathbf{x}) + \sum_{j=1}^k \mathbf{g}_j(\mathbf{x})u_j + \sum_{j=k+1}^{n+m} \mathbf{g}_j(\mathbf{x})(\hat{u}_j + \Delta u_j) + \mathbf{d} + M\mathbf{x}_2 \end{aligned} \quad (2.22)$$

where $\mathbf{g}_j(\mathbf{x})$ is the j -th column of matrix $G(\mathbf{x})$. In order to make the expression more clearly, we redefine some notations, which are a little different form those in the case of passive reliable design. Let $\mathbf{u}_{\mathcal{H}} = (u_1, \dots, u_k)^T$, $\mathbf{u}_{\mathcal{F}} = (u_{k+1}, \dots, u_{n+m})^T$, $\hat{\mathbf{u}}_{\mathcal{F}} = (\hat{u}_{k+1}, \dots, \hat{u}_{n+m})^T$, $\Delta\mathbf{u}_{\mathcal{F}} = (\Delta u_{k+1}, \dots, \Delta u_{n+m})^T$, $G_{\mathcal{H}}(\mathbf{x}) = [\mathbf{g}_1(\mathbf{x}), \dots, \mathbf{g}_k(\mathbf{x})]$ and $G_{\mathcal{F}}(\mathbf{x}) = [\mathbf{g}_{k+1}(\mathbf{x}), \dots, \mathbf{g}_{n+m}(\mathbf{x})]$, then the equation above can be rewritten as

$$\dot{\mathbf{s}} = \mathbf{f}(\mathbf{x}) + G_{\mathcal{H}}(\mathbf{x})\mathbf{u}_{\mathcal{H}} + G_{\mathcal{F}}(\mathbf{x})(\hat{\mathbf{u}}_{\mathcal{F}} + \Delta\mathbf{u}_{\mathcal{F}}) + \mathbf{d} + M\mathbf{x}_2 \quad (2.23)$$

Since the value of $G_{\mathcal{F}}(\mathbf{x})\hat{\mathbf{u}}_{\mathcal{F}}$ was known, this time, we treat $G_{\mathcal{F}}(\mathbf{x})\Delta\mathbf{u}_{\mathcal{F}} + \mathbf{d}$ as a disturbance and impose the following assumption.

Assumption 2.2 There exist nonnegative scalar functions $\sigma_i(\mathbf{x}, t)$, $i = 1, \dots, n$, such that

$$|(G_{\mathcal{F}}(\mathbf{x})\Delta\mathbf{u}_{\mathcal{F}})_i| + |d_i| \leq \sigma_i(\mathbf{x}, t) \quad (2.24)$$

■

It is obviously that the upper bound of $|(G_{\mathcal{F}}(\mathbf{x})\Delta\mathbf{u}_{\mathcal{F}})_i|$ in Assumption 2.2, in general, much less than the one $|(G_{\mathcal{F}}(\mathbf{x})\mathbf{u}_{\mathcal{F}}^*)_i|$ in Assumption 2.1, if the estimate errors $|\Delta u_j|$ are small for $j = k+1, \dots, n+m$. Practically, if the FDD is accurate enough, the error $|\Delta u_j|$ will approach to zero. Utilizing the same design procedures as those of passive reliable design, the VSC laws for those healthy actuators are

$$\mathbf{u}^{eq} = -G_{\mathcal{H}}^T(\mathbf{x}) \left(G_{\mathcal{H}}(\mathbf{x})G_{\mathcal{H}}^T(\mathbf{x}) \right)^{-1} \cdot \{ \mathbf{f}(\mathbf{x}) + G_{\mathcal{F}}(\mathbf{x})\hat{\mathbf{u}}_{\mathcal{F}} + M\mathbf{x}_2 \} \quad (2.25)$$

and

$$\mathbf{u}^{re} = -G_{\mathcal{H}}^T(\mathbf{x}) \left(G_{\mathcal{H}}(\mathbf{x})G_{\mathcal{H}}^T(\mathbf{x}) \right)^{-1} \cdot \{ \Lambda_{\mathcal{H}} \cdot \text{sgn}(\mathbf{s}) \} \quad (2.26)$$

where $\Lambda_{\mathcal{H}} = \text{diag}(\sigma_1(\mathbf{x}, t) + \eta_1, \dots, \sigma_n(\mathbf{x}, t) + \eta_n)$ and $\eta_j > 0$ for $j = 1, \dots, n$, then the overall design input torque is

$$\mathbf{u}_{\mathcal{H}} = \mathbf{u}^{eq} + \mathbf{u}^{re} \quad (2.27)$$

Note that, since the number of healthy actuators are not have to be n ($k \geq n$), implying that there are infinitely solutions for $\mathbf{u}_{\mathcal{H}}$, which the one we used is least norm solution as shown above. If $k = n$, it becomes the same form as that of equation (2.14), except for the $\mathbf{u}_{\mathcal{H}}$ as given by equation (2.27) contain an extra term $G_{\mathcal{F}}(\mathbf{x})\hat{\mathbf{u}}_{\mathcal{F}}$ involving the information of diagnosis. As a result, we can have

$$\begin{aligned} \mathbf{s}^T \dot{\mathbf{s}} &= \mathbf{s}^T \{ G_{\mathcal{F}}(\mathbf{x})\Delta\mathbf{u}_{\mathcal{F}} + \mathbf{d} - \Lambda_{\mathcal{H}} \cdot \text{sgn}(\mathbf{s}) \} \\ &\leq - \sum_{i=1}^n \eta_i \cdot |s_i| \end{aligned} \quad (2.28)$$

by the use of Assumption 2.2, we lead the following result.

Theorem 2.2 Suppose that system (2.1)-(2.2) experiences actuators faults at control channels as given by (2.20) with estimated values and errors given by (2.21). If, in addition, the faults and disturbances satisfy Assumption 2.2, then the origin of system (2.1)-(2.2) is locally asymptotically stable under the control laws given by (2.27). ■

2.3 Reliable Control of Spacecraft Attitude Tracking Problem

2.3.1 Spacecraft Dynamics Analysis

Euler Angles

Before discussing the dynamics of a spacecraft system, we introduce a coordinate transformation [4] first. The orientation of a rigid body with body fixed axes e_1 , e_2 and e_3 associated with unit vectors \hat{e}_1 , \hat{e}_2 and \hat{e}_3 , respectively, can be specified in several ways relative to a reference frame E_1 , E_2 and E_3 associated with unit vectors \hat{E}_1 , \hat{E}_2 and \hat{E}_3 . One of the transformation methods is the classical Euler angles, which is easier to visualize and convenient when working with spinning bodies. When we applied the classical Euler angles to sequential rotations, it has more advantages when only small deviations from the reference frame is involved. Here, we will begin from a two-dimensional sequential rotations, then extend it to a three-dimensional one.

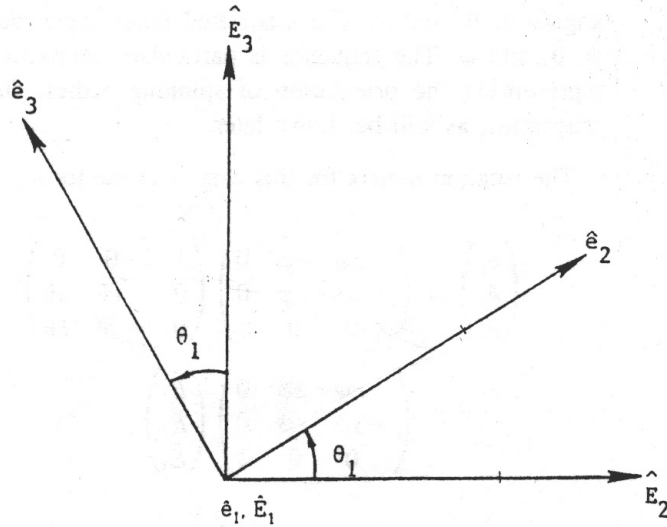


Figure 2.1: An orthogonal rotation in two dimensions

Consider the rotation of a unit orthogonal triad \hat{e}_α through a angle θ_1 relative a reference unit triad \hat{E}_β , where the α and β subscripts take the values of 1, 2, 3 as shown in Figure (2.1). The components of \hat{E}_β along the \hat{e}_α directions are given by

$$\hat{e}_1 = \hat{E}_1$$

$$\hat{e}_2 = \hat{E}_2 \cos \theta_1 + \hat{E}_3 \sin \theta_1$$

$$\hat{e}_3 = -\hat{E}_2 \sin \theta_1 + \hat{E}_3 \cos \theta_1$$

or in matrix form as

$$\begin{pmatrix} \hat{e}_1 \\ \hat{e}_2 \\ \hat{e}_3 \end{pmatrix} = \begin{pmatrix} 1 & 0 & 0 \\ 0 & c\theta_1 & s\theta_1 \\ 0 & -s\theta_1 & c\theta_1 \end{pmatrix} \begin{pmatrix} \hat{E}_1 \\ \hat{E}_2 \\ \hat{E}_3 \end{pmatrix} = R(\theta_1) \begin{pmatrix} \hat{E}_1 \\ \hat{E}_2 \\ \hat{E}_3 \end{pmatrix} \quad (2.29)$$

where c and s denote \cos and \sin function, respectively, and $R(\theta_1)$ is the orthogonal rotation matrix which represents the rotation of the \hat{e}_α unit triad about the \hat{E}_1 unit vector. Similar rotations matrices may be used to represent rotations about other axes.

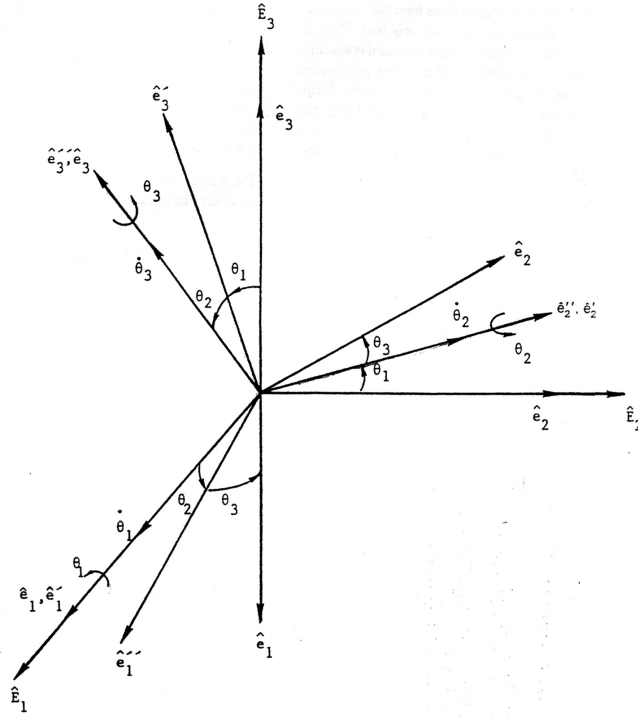


Figure 2.2: An orthogonal rotation in three dimensions

In Figure (2.2), we illustrates sequential θ_1 , θ_2 , θ_3 rotations of the \hat{e}_α unit triad, initially aligned with the \hat{E}_β unit triad, about the \hat{E}_1 (or \hat{e}_1) axis, the rotated \hat{e}_2 (or \hat{e}'_2) and, finally, the rotated \hat{e}_3 (or \hat{e}''_3). Each rotation may be expressed in terms of the orthogonal rotation matrices as follows

$$\begin{pmatrix} \hat{e}'_1 \\ \hat{e}'_2 \\ \hat{e}'_3 \end{pmatrix} = R(\theta_1) \begin{pmatrix} \hat{E}_1 \\ \hat{E}_2 \\ \hat{E}_3 \end{pmatrix}, \quad \begin{pmatrix} \hat{e}''_1 \\ \hat{e}''_2 \\ \hat{e}''_3 \end{pmatrix} = R(\theta_2) \begin{pmatrix} \hat{e}'_1 \\ \hat{e}'_2 \\ \hat{e}'_3 \end{pmatrix}$$

$$\begin{pmatrix} \hat{e}_1 \\ \hat{e}_2 \\ \hat{e}_3 \end{pmatrix} = R(\theta_3) \begin{pmatrix} \hat{e}_1'' \\ \hat{e}_2'' \\ \hat{e}_3'' \end{pmatrix}$$

where

$$R(\theta_1) = \begin{pmatrix} 1 & 0 & 0 \\ 0 & c\theta_1 & s\theta_1 \\ 0 & -s\theta_1 & c\theta_1 \end{pmatrix} \quad R(\theta_2) = \begin{pmatrix} c\theta_2 & 0 & -s\theta_2 \\ 0 & 1 & 0 \\ s\theta_2 & 0 & c\theta_2 \end{pmatrix}$$

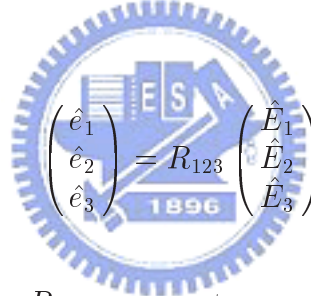
$$R(\theta_3) = \begin{pmatrix} c\theta_3 & s\theta_3 & 0 \\ -s\theta_3 & c\theta_3 & 0 \\ 0 & 0 & 1 \end{pmatrix}$$

The combined matrix for the 1, 2, 3 sequence of rotation is the product of the orthogonal rotation matrices, which is of the form

$$R_{123} = R(\theta_3) \cdot R(\theta_2) \cdot R(\theta_1) =$$

$$\begin{pmatrix} c\theta_2 c\theta_3 & c\theta_3 s\theta_1 s\theta_2 + c\theta_1 s\theta_3 & -c\theta_1 c\theta_3 s\theta_2 + s\theta_1 s\theta_3 \\ -c\theta_2 s\theta_3 & -s\theta_1 s\theta_2 s\theta_3 + c\theta_1 c\theta_3 & c\theta_1 s\theta_2 s\theta_3 + s\theta_1 c\theta_3 \\ s\theta_2 & -c\theta_2 s\theta_1 & c\theta_1 c\theta_2 \end{pmatrix} \quad (2.30)$$

and



$$\begin{pmatrix} \hat{e}_1 \\ \hat{e}_2 \\ \hat{e}_3 \end{pmatrix} = R_{123} \begin{pmatrix} \hat{E}_1 \\ \hat{E}_2 \\ \hat{E}_3 \end{pmatrix} \quad (2.31)$$

The orthogonal rotation matrix R_{123} represents respective reference frames in terms of the rotation angles θ_i . Thus, for a specified vector in the E_β frame is obtained in the e_α frame by evaluating the rotation matrix in equation (2.30) at the rotation angles θ_1 , θ_2 and θ_3 .

Spacecraft Dynamics

Now, we consider the spacecraft dynamics with three actuators in a circular orbit as shown in Figure (2.3). According to the definition of Euler's equation [4], the spacecraft system dynamics, in terms of angular momentum conservation law has the form

$$T + G = \frac{dh}{dt} = \left[\frac{dh}{dt} \right]_b + \omega \times h, \quad (2.32)$$

where T denotes external disturbance (including solar pressure torque, magnetic field disturbance and external input torque), G is the gravity gradient torque due to the earth,

h is the total angular momentum, ω is the angular rate of the body coordinate frame of the spacecraft, and the symbol $[\cdot]_b$ means that it is with respect to the body coordinate frame itself. Here, we redefine the three standard basis vectors of the spacecraft body coordinate frame \hat{e}_1, \hat{e}_2 and \hat{e}_3 in Figure (2.3) as $\hat{e}_x = \hat{e}_3, \hat{e}_y = \hat{e}_2$ and $\hat{e}_z = \hat{e}_1$, which are the three unit vectors in x, y and z axes of the orthogonal coordinate, respectively. Thus, the total angular momentum can be expressed as

$$h = (I_x\omega_x + h_{wx})\hat{e}_x + (I_y\omega_y + h_{wy})\hat{e}_y + (I_z\omega_z + h_{wz})\hat{e}_z \quad (2.33)$$

where I_x, I_y, I_z are the inertia of the spacecraft body, $\omega_x, \omega_y, \omega_z$ are the angular rates

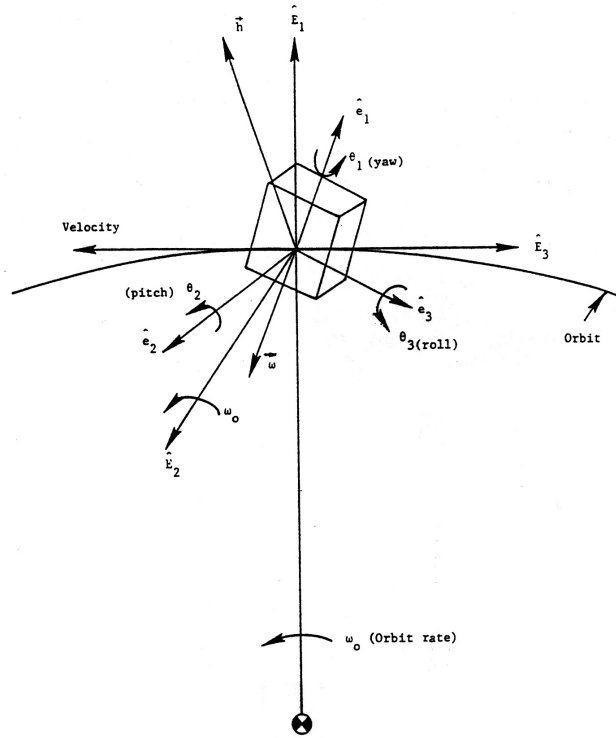


Figure 2.3: Spacecraft on the orbit

with respect to x, y , and z axes, and h_{wx}, h_{wy}, h_{wz} are the inertia of the three reaction wheels in x, y , and z directions, respectively. Substituting equations (2.33) into (2.32), we have

$$T + G = \begin{pmatrix} I_x\dot{\omega}_x + \dot{h}_{wx} + (I_z - I_y)\omega_y\omega_z + \omega_y h_{wz} - \omega_z h_{wy} \\ I_y\dot{\omega}_y + \dot{h}_{wy} + (I_x - I_z)\omega_x\omega_z + \omega_z h_{wx} - \omega_x h_{wz} \\ I_z\dot{\omega}_z + \dot{h}_{wz} + (I_y - I_x)\omega_x\omega_y + \omega_x h_{wy} - \omega_y h_{wx} \end{pmatrix} \quad (2.34)$$

then according to [4], the angular rate and Euler angles have the following relation

$$\omega_\alpha = \dot{\theta}_\alpha + \omega_0 E_2 \cdot e_\alpha, \quad \alpha = x, y, z \quad (2.35)$$

Define ϕ (θ_x), θ (θ_y), and ψ (θ_z) are the rotational angles with respect to x , y and z axis, respectively, from the spacecraft body coordinate frame to orbit coordinate frame, E_2 is the unit vector of orbit coordinate frame which perpendicular to the orbit plane as shown in Figure (2.3), and ω_0 is the constant orbit rate of the spacecraft with fixed speed in a circular orbit. Taking equation (2.30) into (2.35), then the equation (2.35) can be revealed as the form

$$\omega = \begin{pmatrix} \omega_x \\ \omega_y \\ \omega_z \end{pmatrix} = \begin{pmatrix} \dot{\phi} - \omega_0 \sin \psi \cos \theta \\ \dot{\theta} + \omega_0 (\cos \psi \cos \phi - \sin \psi \sin \theta \sin \phi) \\ \dot{\psi} + \omega_0 (\cos \psi \sin \phi + \cos \phi \sin \psi \sin \theta) \end{pmatrix} \quad (2.36)$$

form [4], the gravity gradient torque is

$$G = \begin{pmatrix} G_x \\ G_y \\ G_z \end{pmatrix} = \begin{pmatrix} -3/2\omega_0^2(I_y - I_z) \cos^2 \theta \sin 2\phi \\ 3/2\omega_0^2(I_z - I_x) \sin 2\theta \cos \phi \\ -3/2\omega_0^2(I_x - I_y) \sin 2\theta \sin \phi \end{pmatrix} \quad (2.37)$$

and the external disturbance

$$T = \begin{pmatrix} T_x \\ T_y \\ T_z \end{pmatrix} \quad (2.38)$$

Here, we ignore the solar pressure torque and magnetic field disturbance, and regard T_x , T_y and T_z as the thruster inputs, which are the only control force we applied. After combining equations (2.36), (2.37) and (2.38) with (2.34), and define the state variables as $x_1 = \phi$, $x_2 = \dot{\phi}$, $x_3 = \theta$, $x_4 = \dot{\theta}$, $x_5 = \psi$, and $x_6 = \dot{\psi}$, the spacecraft dynamics can be represented in the form of

$$\dot{x} = f(x) + g(x)u \quad (2.39)$$

with $x = (x_1 \ x_2 \ x_3 \ x_4 \ x_5 \ x_6)^T$, $u = (T_x/I_x, T_y/I_y, T_z/I_z)^T$ and $f(x) = (f_1 \ f_2 \ f_3 \ f_4 \ f_5 \ f_6)^T$, where

$$f_1 = x_2 \quad (2.40)$$

$$f_3 = x_4 \quad (2.41)$$

$$f_5 = x_6 \quad (2.42)$$

$$\begin{aligned} f_2 = & \omega_0 x_6 c x_5 c x_3 - \omega_0 x_4 s x_5 s x_3 + (I_y - I_z)/I_x [x_4 x_6 + \omega_0 x_4 c x_1 s x_5 s x_3 + \omega_0 x_4 c x_5 s x_1 \\ & + \omega_0 x_6 c x_5 c x_1 + \frac{1}{2} \omega_0^2 s(2x_5) c^2 x_1 s x_3 + \frac{1}{2} \omega_0^2 c^2 x_5 s(2x_1) - \omega_0 x_6 s x_5 s x_3 s x_1 \\ & - \frac{1}{2} \omega_0^2 s^2 x_3 s^2 x_5 s(2x_1) - \frac{1}{2} \omega_0^2 s(2x_5) s x_3 s^2 x_1 - \frac{3}{2} \omega_0^2 c^2 x_3 s(2x_1)] + 1/I_x [-\dot{h}_{\omega x} \\ & - h_{\omega z} (x_4 + \omega_0 c x_5 c x_1 - \omega_0 s x_5 s x_3 s x_1) + h_{\omega y} (x_6 + \omega_0 c x_1 s x_5 s x_3 + \omega_0 c x_5 s x_1)] \end{aligned} \quad (2.43)$$

$$\begin{aligned} f_4 = & \omega_0 x_6 s x_5 c x_1 + \omega_0 x_2 c x_5 s x_1 + \omega_0 x_6 c x_5 s x_3 s x_1 + \omega_0 x_4 s x_5 c x_3 s x_1 + \omega_0 x_2 s x_5 s x_3 c x_1 \\ & + (I_z - I_x)/I_y [x_2 x_6 + \omega_0 x_2 c x_1 s x_5 s x_3 + \omega_0 x_2 c x_5 s x_1 - \omega_0 x_6 c x_5 c x_3 \\ & - \frac{1}{2} \omega_0^2 s(2x_3) s^2 x_5 c x_1 - \frac{1}{2} \omega_0^2 s(2x_5) c x_3 s x_1 + \frac{3}{2} \omega_0^2 s(2x_3) c x_1] + 1/I_y [-\dot{h}_{\omega y} \\ & - h_{\omega x} (x_6 + \omega_0 c x_1 s x_5 s x_3 + \omega_0 c x_5 s x_1) + h_{\omega z} (x_2 - \omega_0 s x_5 c x_3)] \end{aligned} \quad (2.44)$$

$$\begin{aligned} f_6 = & \omega_0 x_2 s x_1 s x_5 s x_3 - \omega_0 x_6 c x_1 c x_5 s x_3 - \omega_0 x_4 c x_1 s x_5 c x_3 + \omega_0 x_6 s x_5 s x_1 - \omega_0 x_2 c x_5 c x_1 \\ & + (I_x - I_y)/I_z [x_2 x_4 + \omega_0 x_2 c x_5 c x_1 - \omega_0 x_2 s x_5 s x_3 s x_1 - \omega_0 x_4 s x_5 c x_3 \\ & - \frac{1}{2} \omega_0^2 s(2x_5) c x_3 c x_1 + \frac{1}{2} \omega_0^2 s^2 x_5 s x_1 s(2x_3) - \frac{3}{2} \omega_0^2 s(2x_3) s x_1] + 1/I_z [-\dot{h}_{\omega z} \\ & - h_{\omega y} (x_2 - \omega_0 s x_5 c x_3) + h_{\omega x} (x_4 + \omega_0 c x_5 c x_1 - \omega_0 s x_5 s x_3 s x_1)] \end{aligned} \quad (2.45)$$

and

$$g(x) = \begin{pmatrix} 0 & 0 & 0 \\ 1 & 0 & 0 \\ 0 & 0 & 0 \\ 0 & 1 & 0 \\ 0 & 0 & 0 \\ 0 & 0 & 1 \end{pmatrix} \quad (2.46)$$

similarly, c and s denote *cos* and *sin* function, respectively.

Note that, the above spacecraft dynamics is primarily depicted for three control inputs, however, in many practical applications, a system often equips with redundancy to allow safe operation when some of the actuators experience faults. An example can be found in the design of ROCSAT II satellite [28] which is equipped with four actuators. The connection between the three and four actuators (see Figure (2.4)) in ROCSAT II is

through the transformation matrix

$$S = \begin{pmatrix} 0.67 & 0.67 & 0.67 & 0.67 \\ 0.69 & -0.69 & -0.69 & 0.69 \\ 0.28 & 0.28 & -0.28 & -0.28 \end{pmatrix}_{3 \times 4} \quad (2.47)$$

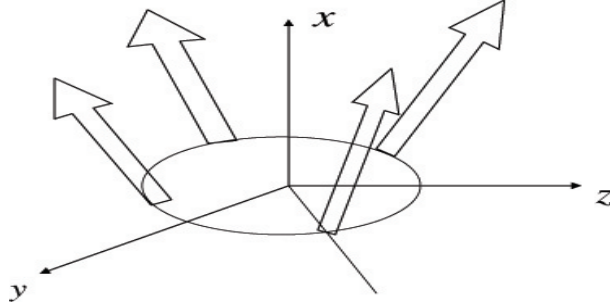


Figure 2.4: Transformation representation

Therefore, the dynamics (2.39) can be rewritten as the form

$$\dot{x} = f(x) + \bar{g}(x)\bar{u} \quad (2.48)$$

where the function $f(x)$ is the same as those in equations (2.40)-(2.45), and $\bar{g}(x)$ and \bar{u} have the form

$$\bar{g}(x) = \begin{pmatrix} 0 & 0 & 0 & 0 \\ 0.67 & 0.67 & 0.67 & 0.67 \\ 0 & 0 & 0 & 0 \\ 0.69 & -0.69 & -0.69 & 0.69 \\ 0 & 0 & 0 & 0 \\ 0.28 & 0.28 & -0.28 & -0.28 \end{pmatrix} \quad (2.49)$$

$$\bar{u} = \begin{pmatrix} u_1 \\ u_2 \\ u_3 \\ u_4 \end{pmatrix} \quad (2.50)$$

here, u_1, u_2, u_3 and u_4 are the control torque in four directions of ROCSAT II.

Integrating the discussions about spacecraft system above, in order to make the illustrations of FDD and reliable control designs in later sections more clearly, we rearrange the state variables of spacecraft dynamics as the form similar to equations (2.1)-(2.2), that is $\mathbf{x}_1 = (x_1, x_3, x_5)^T$ and $\mathbf{x}_2 = (x_2, x_4, x_6)^T$, where

$$\dot{\mathbf{x}}_1 = \mathbf{x}_2 \quad (2.51)$$

$$\dot{\mathbf{x}}_2 = \begin{pmatrix} f_2 \\ f_4 \\ f_6 \end{pmatrix} + \begin{pmatrix} 0.67 & 0.67 & 0.67 & 0.67 \\ 0.69 & -0.69 & -0.69 & 0.69 \\ 0.28 & 0.28 & -0.28 & -0.28 \end{pmatrix} \mathbf{u} \quad (2.52)$$

where f_2 , f_4 and f_6 are system parameters of spacecraft system as shown in equation (2.40)-(2.45), $G(\mathbf{x})$ is a 3×4 matrix where the three rows of it are the 2-th, 4-th, and 6-th row of $\bar{g}(x)$, respectively, $\mathbf{u} = (u_1, u_2, u_3, u_4)^T$ is the same as \bar{u} of equation (2.50), and this representation will be used throughout this thesis.

2.3.2 Fault Detection and Diagnosis (FDD) Observer Design

Problem Formulation

In this section, we consider the nonlinear system as given by

$$\dot{\mathbf{x}}_1 = \mathbf{x}_2 \quad (2.53)$$

$$\dot{\mathbf{x}}_2 = \mathbf{f}(\mathbf{x}) + G(\mathbf{x})\mathbf{u}, \quad \mathbf{f}(\mathbf{0}) = \mathbf{0} \quad (2.54)$$

where $\mathbf{f}(\mathbf{x})$ and $G(\mathbf{x})$ are assumed to be smooth. The main goal of this section is to design an observer that can real-time detect the occurrence of actuator outage and diagnose the location of fault. The configuration of the FDD system is described in Figure (2.5).

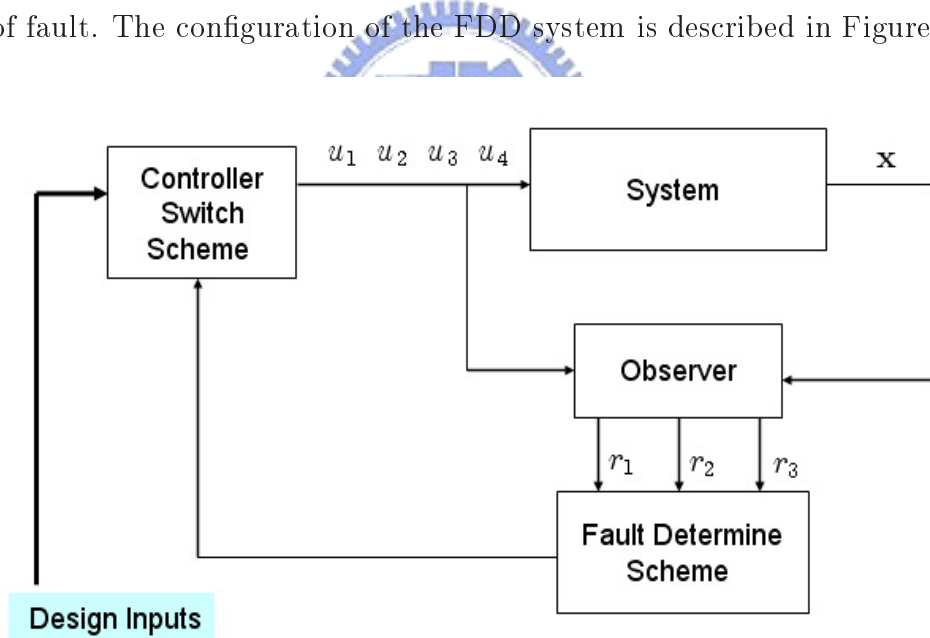


Figure 2.5: FDD configuration

The Transformation of Decoupled Form

From the spacecraft system dynamics (2.51)-(2.52), the system has six states $\mathbf{x} = (x_1, x_3, x_5, x_2, x_4, x_6)^T$. We assume that all the states are measurable and rewrite equations

(2.51)-(2.52) into the following form

$$\dot{\mathbf{x}}_1 = \mathbf{x}_2 \quad (2.55)$$

$$\dot{\mathbf{x}}_2 = \begin{pmatrix} f_2 \\ f_4 \\ f_6 \end{pmatrix} + \begin{pmatrix} g_{11} & g_{12} & g_{13} & g_{14} \\ g_{21} & g_{22} & g_{23} & g_{24} \\ g_{31} & g_{32} & g_{33} & g_{34} \end{pmatrix} \begin{pmatrix} u_1 \\ u_2 \\ u_3 \\ u_4 \end{pmatrix} \quad (2.56)$$

The reason we rewrite equations (2.51)-(2.52) to the form (2.55)-(2.56) is that the transformation we are going to introduce can be applied not only onto the spacecraft model, but also other systems which has the same form, and the only condition is that any combination of three of the four columns of $G(\mathbf{x})$ is nonsingular.

It is clear from (2.55)-(2.56) that the four actuator inputs only appear in the state equations \dot{x}_2, \dot{x}_4 and \dot{x}_6 . In order to decouple the actuator faults, we make the following state transformation

$$\mathbf{z} = P\mathbf{x}_2 \quad (2.57)$$

with

$$P = \begin{pmatrix} g_{11} & g_{12} & g_{13} \\ g_{21} & g_{22} & g_{23} \\ g_{31} & g_{32} & g_{33} \end{pmatrix}^{-1} \quad (2.58)$$

and the matrix P is assumed to be nonsingular, then state equations in new state variables are described as

$$\dot{\mathbf{z}} = \mathbf{f}_{new} + PG(\mathbf{x})\mathbf{u} \quad (2.59)$$

where \mathbf{f}_{new} and $PG(\mathbf{x})$ are given by

$$\mathbf{f}_{new} = P\mathbf{f}(\mathbf{x}) = \begin{pmatrix} f_{1\ new} \\ f_{2\ new} \\ f_{3\ new} \end{pmatrix} \quad (2.60)$$

$$PG(\mathbf{x}) = \begin{pmatrix} 1 & 0 & 0 & l_1 \\ 0 & 1 & 0 & l_2 \\ 0 & 0 & 1 & l_3 \end{pmatrix} \quad (2.61)$$

under these settings, we have

$$\dot{z}_1 = f_{1\ new} + u_1 + l_1 u_4 \quad (2.62)$$

$$\dot{z}_2 = f_{2\ new} + u_2 + l_2 u_4 \quad (2.63)$$

$$\dot{z}_3 = f_{3\ new} + u_3 + l_3 u_4 \quad (2.64)$$

Clearly, z_1 is only affected by actuators u_1 and u_4 , similarly, z_2 is affected by actuators u_2 and u_4 , and z_3 is affected by actuators u_3 and u_4 . Because any two actuators fail at the same time, the tracking maneuvers cannot be achieved, thus, we only consider the case of single actuator outage.

Observer Design

With the aid of transformed system (2.62)-(2.64), we design the observer (ξ_i) and residual signals (r_i) as follows

$$\dot{\xi}_1 = f_{1\ new} + u_1 + l_1 u_4 + k_1(z_1 - \xi_1) \quad (2.65)$$

$$\dot{\xi}_2 = f_{2\ new} + u_2 + l_2 u_4 + k_2(z_2 - \xi_2) \quad (2.66)$$

$$\dot{\xi}_3 = f_{3\ new} + u_3 + l_3 u_4 + k_3(z_3 - \xi_3) \quad (2.67)$$

and

$$r_1 = z_1 - \xi_1 \quad (2.68)$$

$$r_2 = z_2 - \xi_2 \quad (2.69)$$

$$r_3 = z_3 - \xi_3 \quad (2.70)$$

where u_1 , u_2 , u_3 and u_4 in observer equations (2.65)-(2.67) are designed torque in normal operation and $k_i > 0$, for $i = 1, 2, 3$. Under this design, we claim that any single actuator outage can be detected and diagnosed. Indeed, it is shown later the outage of the first actuator u_1 results in $|r_1| \neq 0$ but $|r_2| = |r_3| = 0$, the outage of the second actuator u_2 leads to $|r_2| \neq 0$ but $|r_1| = |r_3| = 0$, the outage of the third actuator u_3 gives rise to $|r_3| \neq 0$ but $|r_1| = |r_2| = 0$, and finally, the outage of the fourth actuator u_4 gives $|r_1| \neq 0$, $|r_2| \neq 0$ and $|r_3| \neq 0$. To see this, suppose that the first actuator experiences fault with

actual value u_1^* , and define

$$m_1 = u_1^* - u_1 \quad (2.71)$$

where u_1 is designed value, and m_1 is the fault signal between actual and designed values of actuator u_1 , then the equation (2.62) becomes

$$\begin{aligned} \dot{z}_1 &= f_{1 \text{ new}} + u_1^* + l_1 u_4 \\ &= f_{1 \text{ new}} + u_1 + l_1 u_4 + m_1 \end{aligned} \quad (2.72)$$

It follows from the equations (2.62), (2.65) and (2.68) that

$$\begin{aligned} \dot{r}_1 &= \dot{z}_1 - \dot{\xi}_1 \\ &= -k_1 r_1 + m_1 \end{aligned} \quad (2.73)$$

Since k_1 is assumed to be a positive constant, r_1 will approach to m_1/k_1 after a short time transient. Thus, the residual signal r_1 is affected by the fault signal m_1 , that is

$$m_1 \neq 0 \Rightarrow r_1 \neq 0 \quad (2.74)$$

By similar methods, we define the fault signals of u_2 , u_3 and u_4 are m_2 , m_3 and m_4 , respectively, thus we can get

$$m_2 \neq 0 \Rightarrow r_2 \neq 0$$

$$m_3 \neq 0 \Rightarrow r_3 \neq 0$$

$$m_4 \neq 0 \Rightarrow r_1, r_2, r_3 \neq 0$$

2.3.3 Reliable VSC Controller Design

In this section, we employ the VSC scheme to design the reliable controller for the spacecraft to achieve the attitude stabilization even when a specific actuator experiences abnormal operation. From equations (2.51)-(2.52), we know that the system has six states and four inputs. That is, x_1 , x_3 and x_5 are the rotational angles in x , y and z directions, respectively, and x_2 , x_4 and x_6 are corresponding angular rates. Let $G(\mathbf{x}) = (\mathbf{g}_1 \ \mathbf{g}_2 \ \mathbf{g}_3 \ \mathbf{g}_4)$, where \mathbf{g}_i , for $i = 1, \dots, 4$, are four columns of $G(\mathbf{x})$, respectively, and any combination of three of them is linearly independent. Our goal here is to stabilize the spacecraft at a

specified attitude as desired. To this end, we define the desired angles of x_1 , x_3 and x_5 as x_{1d} , x_{3d} and x_{5d} , respectively, and define the attitude error as

$$\mathbf{e} = \begin{pmatrix} e_1 \\ e_2 \\ e_3 \end{pmatrix} = \begin{pmatrix} x_1 - x_{1d} \\ x_3 - x_{3d} \\ x_5 - x_{5d} \end{pmatrix} \quad (2.75)$$

then select the sliding surface to be

$$\mathbf{s} = \dot{\mathbf{e}} + M\mathbf{e} = 0$$

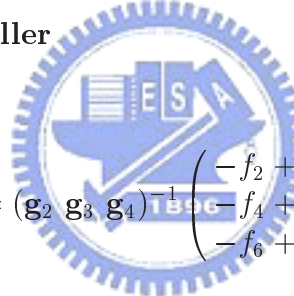
or in the form

$$\mathbf{s} = \begin{pmatrix} s_1 \\ s_2 \\ s_3 \end{pmatrix} = \begin{pmatrix} \dot{e}_1 + m_{11}e_1 \\ \dot{e}_2 + m_{22}e_2 \\ \dot{e}_3 + m_{33}e_3 \end{pmatrix} \quad (2.76)$$

where the positive definite matrix M we use here is a 3×3 diagonal one and the elements on the line are m_{11} , m_{22} and m_{33} . Following the reliable control design procedures discussed in Section 2.2, the passive and active reliable controller are given below

A. Passive Reliable Controller

(a) design for u_1 outage



$$\begin{pmatrix} u_2^{eq} \\ u_3^{eq} \\ u_4^{eq} \end{pmatrix} = (\mathbf{g}_2 \ \mathbf{g}_3 \ \mathbf{g}_4)^{-1} \begin{pmatrix} -f_2 + \ddot{x}_{1d} - m_{11}\dot{e}_1 \\ -f_4 + \ddot{x}_{3d} - m_{22}\dot{e}_2 \\ -f_6 + \ddot{x}_{5d} - m_{33}\dot{e}_3 \end{pmatrix}$$

$$\begin{pmatrix} u_2^{re} \\ u_3^{re} \\ u_4^{re} \end{pmatrix} = (\mathbf{g}_2 \ \mathbf{g}_3 \ \mathbf{g}_4)^{-1} \begin{pmatrix} -(\rho_1 + \eta_1) \cdot \text{sgn}(s_1) \\ -(\rho_2 + \eta_2) \cdot \text{sgn}(s_2) \\ -(\rho_3 + \eta_3) \cdot \text{sgn}(s_3) \end{pmatrix}$$

$$u_1^{eq} = 0 \quad \text{and} \quad u_1^{re} = -\eta_4 \cdot \text{sgn}(\mathbf{g}_1^T \mathbf{s})$$

(b) design for u_2 outage

$$\begin{pmatrix} u_1^{eq} \\ u_3^{eq} \\ u_4^{eq} \end{pmatrix} = (\mathbf{g}_1 \ \mathbf{g}_3 \ \mathbf{g}_4)^{-1} \begin{pmatrix} -f_2 + \ddot{x}_{1d} - m_{11}\dot{e}_1 \\ -f_4 + \ddot{x}_{3d} - m_{22}\dot{e}_2 \\ -f_6 + \ddot{x}_{5d} - m_{33}\dot{e}_3 \end{pmatrix}$$

$$\begin{pmatrix} u_1^{re} \\ u_3^{re} \\ u_4^{re} \end{pmatrix} = (\mathbf{g}_1 \ \mathbf{g}_3 \ \mathbf{g}_4)^{-1} \begin{pmatrix} -(\rho_1 + \eta_1) \cdot \text{sgn}(s_1) \\ -(\rho_2 + \eta_2) \cdot \text{sgn}(s_2) \\ -(\rho_3 + \eta_3) \cdot \text{sgn}(s_3) \end{pmatrix}$$

$$u_2^{eq} = 0 \quad \text{and} \quad u_2^{re} = -\eta_4 \cdot \text{sgn}(\mathbf{g}_2^T \mathbf{s})$$

(c) design for u_3 outage

$$\begin{pmatrix} u_1^{eq} \\ u_2^{eq} \\ u_4^{eq} \end{pmatrix} = (\mathbf{g}_1 \ \mathbf{g}_2 \ \mathbf{g}_4)^{-1} \begin{pmatrix} -f_2 + \ddot{x}_{1d} - m_{11}\dot{e}_1 \\ -f_4 + \ddot{x}_{3d} - m_{22}\dot{e}_2 \\ -f_6 + \ddot{x}_{5d} - m_{33}\dot{e}_3 \end{pmatrix}$$

$$\begin{pmatrix} u_1^{re} \\ u_2^{re} \\ u_4^{re} \end{pmatrix} = (\mathbf{g}_1 \ \mathbf{g}_2 \ \mathbf{g}_4)^{-1} \begin{pmatrix} -(\rho_1 + \eta_1) \cdot \text{sgn}(s_1) \\ -(\rho_2 + \eta_2) \cdot \text{sgn}(s_2) \\ -(\rho_3 + \eta_3) \cdot \text{sgn}(s_3) \end{pmatrix}$$

$$u_3^{eq} = 0 \quad \text{and} \quad u_3^{re} = -\eta_4 \cdot \text{sgn}(\mathbf{g}_3^T \mathbf{s})$$

(d) design for u_4 outage

$$\begin{pmatrix} u_1^{eq} \\ u_2^{eq} \\ u_3^{eq} \end{pmatrix} = (\mathbf{g}_1 \ \mathbf{g}_2 \ \mathbf{g}_3)^{-1} \begin{pmatrix} -f_2 + \ddot{x}_{1d} - m_{11}\dot{e}_1 \\ -f_4 + \ddot{x}_{3d} - m_{22}\dot{e}_2 \\ -f_6 + \ddot{x}_{5d} - m_{33}\dot{e}_3 \end{pmatrix}$$

$$\begin{pmatrix} u_1^{re} \\ u_2^{re} \\ u_3^{re} \end{pmatrix} = (\mathbf{g}_1 \ \mathbf{g}_2 \ \mathbf{g}_3)^{-1} \begin{pmatrix} -(\rho_1 + \eta_1) \cdot \text{sgn}(s_1) \\ -(\rho_2 + \eta_2) \cdot \text{sgn}(s_2) \\ -(\rho_3 + \eta_3) \cdot \text{sgn}(s_3) \end{pmatrix}$$

$$u_4^{eq} = 0 \quad \text{and} \quad u_4^{re} = -\eta_4 \cdot \text{sgn}(\mathbf{g}_4^T \mathbf{s})$$

B. Active Reliable Controller

(a) when normal operation

$$\begin{pmatrix} u_1^{eq} \\ u_2^{eq} \\ u_3^{eq} \\ u_4^{eq} \end{pmatrix} = G^T(\mathbf{x}) \left(G(\mathbf{x})G^T(\mathbf{x}) \right)^{-1} \begin{pmatrix} -f_2 + \ddot{x}_{1d} - m_{11}\dot{e}_1 \\ -f_4 + \ddot{x}_{3d} - m_{22}\dot{e}_2 \\ -f_6 + \ddot{x}_{5d} - m_{33}\dot{e}_3 \end{pmatrix}$$

$$\begin{pmatrix} u_1^{re} \\ u_2^{re} \\ u_3^{re} \\ u_4^{re} \end{pmatrix} = G^T(\mathbf{x}) \left(G(\mathbf{x})G^T(\mathbf{x}) \right)^{-1} \begin{pmatrix} -(\sigma_1 + \eta_1) \cdot \text{sgn}(s_1) \\ -(\sigma_2 + \eta_2) \cdot \text{sgn}(s_2) \\ -(\sigma_3 + \eta_3) \cdot \text{sgn}(s_3) \end{pmatrix}$$

(b) when u_1 outage

$$\begin{pmatrix} u_2^{eq} \\ u_3^{eq} \\ u_4^{eq} \end{pmatrix} = (\mathbf{g}_2 \ \mathbf{g}_3 \ \mathbf{g}_4)^{-1} \begin{pmatrix} -f_2 + \ddot{x}_{1d} - m_{11}\dot{e}_1 - g_{11}\hat{u}_1 \\ -f_4 + \ddot{x}_{3d} - m_{22}\dot{e}_2 - g_{21}\hat{u}_1 \\ -f_6 + \ddot{x}_{5d} - m_{33}\dot{e}_3 - g_{31}\hat{u}_1 \end{pmatrix}$$

$$\begin{pmatrix} u_2^{re} \\ u_3^{re} \\ u_4^{re} \end{pmatrix} = (\mathbf{g}_2 \ \mathbf{g}_3 \ \mathbf{g}_4)^{-1} \begin{pmatrix} -(\sigma_1 + \eta_1) \cdot \text{sgn}(s_1) \\ -(\sigma_2 + \eta_2) \cdot \text{sgn}(s_2) \\ -(\sigma_3 + \eta_3) \cdot \text{sgn}(s_3) \end{pmatrix}$$

(c) when u_2 outage

$$\begin{pmatrix} u_1^{eq} \\ u_3^{eq} \\ u_4^{eq} \end{pmatrix} = (\mathbf{g}_1 \ \mathbf{g}_3 \ \mathbf{g}_4)^{-1} \begin{pmatrix} -f_2 + \ddot{x}_{1d} - m_{11}\dot{e}_1 - g_{12}\hat{u}_2 \\ -f_4 + \ddot{x}_{3d} - m_{22}\dot{e}_2 - g_{22}\hat{u}_2 \\ -f_6 + \ddot{x}_{5d} - m_{33}\dot{e}_3 - g_{32}\hat{u}_2 \end{pmatrix}$$

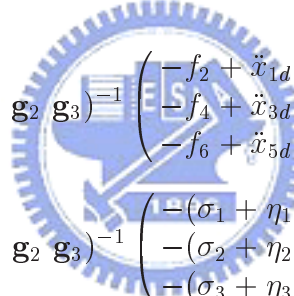
$$\begin{pmatrix} u_1^{re} \\ u_3^{re} \\ u_4^{re} \end{pmatrix} = (\mathbf{g}_1 \ \mathbf{g}_3 \ \mathbf{g}_4)^{-1} \begin{pmatrix} -(\sigma_1 + \eta_1) \cdot \text{sgn}(s_1) \\ -(\sigma_2 + \eta_2) \cdot \text{sgn}(s_2) \\ -(\sigma_3 + \eta_3) \cdot \text{sgn}(s_3) \end{pmatrix}$$

(d) when u_3 outage

$$\begin{pmatrix} u_1^{eq} \\ u_2^{eq} \\ u_4^{eq} \end{pmatrix} = (\mathbf{g}_1 \ \mathbf{g}_2 \ \mathbf{g}_4)^{-1} \begin{pmatrix} -f_2 + \ddot{x}_{1d} - m_{11}\dot{e}_1 - g_{13}\hat{u}_3 \\ -f_4 + \ddot{x}_{3d} - m_{22}\dot{e}_2 - g_{23}\hat{u}_3 \\ -f_6 + \ddot{x}_{5d} - m_{33}\dot{e}_3 - g_{33}\hat{u}_3 \end{pmatrix}$$

$$\begin{pmatrix} u_1^{re} \\ u_2^{re} \\ u_4^{re} \end{pmatrix} = (\mathbf{g}_1 \ \mathbf{g}_2 \ \mathbf{g}_4)^{-1} \begin{pmatrix} -(\sigma_1 + \eta_1) \cdot \text{sgn}(s_1) \\ -(\sigma_2 + \eta_2) \cdot \text{sgn}(s_2) \\ -(\sigma_3 + \eta_3) \cdot \text{sgn}(s_3) \end{pmatrix}$$

(e) when u_4 outage



$$\begin{pmatrix} u_1^{eq} \\ u_2^{eq} \\ u_3^{eq} \end{pmatrix} = (\mathbf{g}_1 \ \mathbf{g}_2 \ \mathbf{g}_3)^{-1} \begin{pmatrix} -f_2 + \ddot{x}_{1d} - m_{11}\dot{e}_1 - g_{14}\hat{u}_4 \\ -f_4 + \ddot{x}_{3d} - m_{22}\dot{e}_2 - g_{24}\hat{u}_4 \\ -f_6 + \ddot{x}_{5d} - m_{33}\dot{e}_3 - g_{34}\hat{u}_4 \end{pmatrix}$$

$$\begin{pmatrix} u_1^{re} \\ u_2^{re} \\ u_3^{re} \end{pmatrix} = (\mathbf{g}_1 \ \mathbf{g}_2 \ \mathbf{g}_3)^{-1} \begin{pmatrix} -(\sigma_1 + \eta_1) \cdot \text{sgn}(s_1) \\ -(\sigma_2 + \eta_2) \cdot \text{sgn}(s_2) \\ -(\sigma_3 + \eta_3) \cdot \text{sgn}(s_3) \end{pmatrix}$$

where \hat{u}_i , for $i = 1, 2, 3, 4$ are the fault values of input torque detected by FDD, ρ_i and σ_i , for $i = 1, 2, 3$ satisfy Assumptions 2.1 and 2.2, respectively.

2.3.4 Simulation Results

Here, we display the tracking performances of passive and active reliable VSC controls of a spacecraft with thrusters as control inputs. In the simulations, the parameters of spacecraft are chosen as $I_x = I_z = 2000N \cdot m \cdot s^2$ and $I_y = 400N \cdot m \cdot s^2$ (spacecraft is symmetric with y-axis) and orbit rate $\omega_0 = 1.032 \times 10^{-3}rad/s$. The parameters of VSC schemes for both passive and active designs are selected as $m_{11} = m_{22} = m_{33} = 2$, $\eta_i = 0.4$, for $i = 1, 2, 3, 4$ and the sign function is replaced by the saturation function with boundary layer width $\epsilon_i = 0.05$, for $i = 1, 2, 3$. FDD parameters of active designs

are set to $k_i = 10$, for $i = 1, 2, 3$, and the alarms are fired if $|r_i| \geq 0.01$. For practical situation, we constraint that the input torque u_i , for $i = 1, 2, 3, 4$ can not exceed one. Base on those settings, we know the boundary of alarms is 10 percent of maximum input torque ($0.01 = |r_i| = \frac{m_i}{k_i} = \frac{0.1}{10}$), whenever there is an alarm, the associated active reliable controller is then activated according to FDD information. To show the performances, we list four items for each case, which are

- (1) T_{con} : The last time for all states are converge within 0.01 from the desired ones.
- (2) $f \mathbf{x}^T \mathbf{x} + \mathbf{u}^T \mathbf{u}$: Quadratic performance of states and torques.
- (3) $f \mathbf{u}^T \mathbf{u}$: Required energy.
- (4) $\|\mathbf{u}\|_\infty$: Maximum input torque.

and the situation we simulate is from the initial state $\mathbf{x}(0) = (-0.7, -0.07, 1.5, 0.3, 1.3, -0.2)^T$ to the desired attitude $\mathbf{x}_d(t) \equiv \mathbf{0}$.

Numerical simulations are summarized in Tables (2.1) and (2.2). For passive VSC control, we only show the design with regard to u_2 as the susceptible actuator, and simulate the situations of normal operation, and u_1, u_2, u_3 and u_4 are experience faults. For active ones, the control will be switched according to the information of FDD. In these tables, condition Normal means normal operation, while u_1, u_2, u_3 and u_4 imply that the associated input experience faults at one second, respectively, and the notation X means that the system states do not converge, as a result, the performance are not meaningful anymore. The graphs of states and input torque of passive reliable controls are shown in Figure (2.6) to Figure (2.10), and the associated graphs of active ones are shown in Figure (2.11) to Figure (2.15). Note that, the notations a_1, a_2 , and a_3 are alarm1, alarm2, and alarm3 of corresponding residual r_1, r_2 and r_3 , respectively.

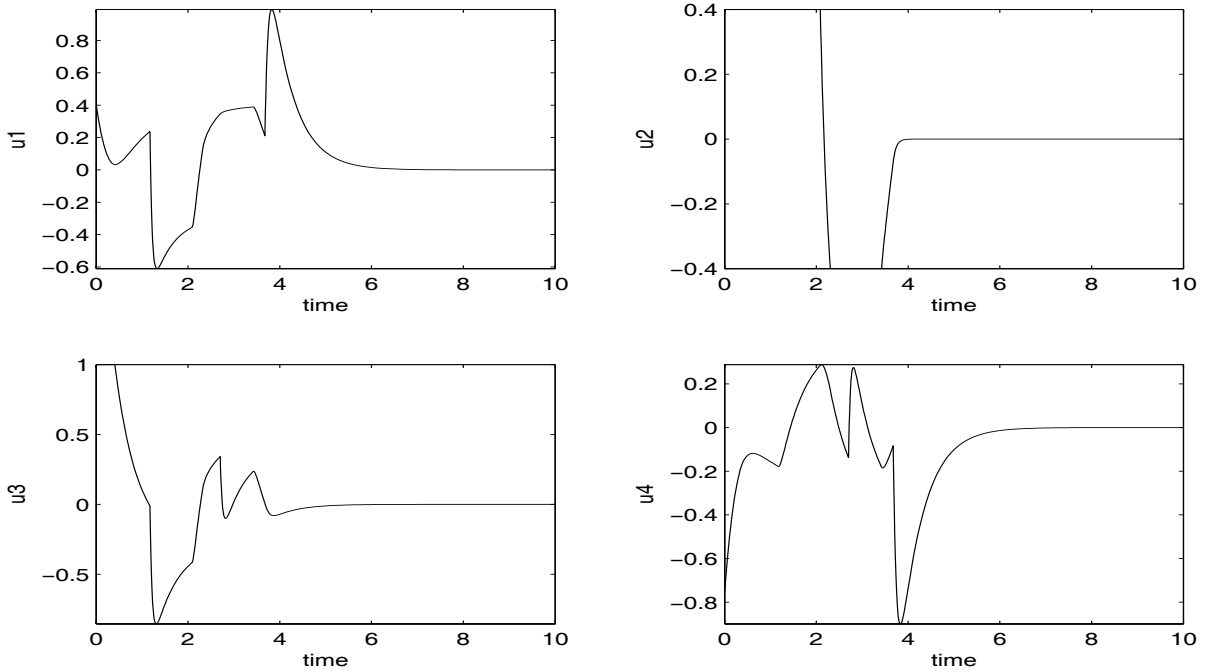
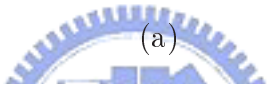
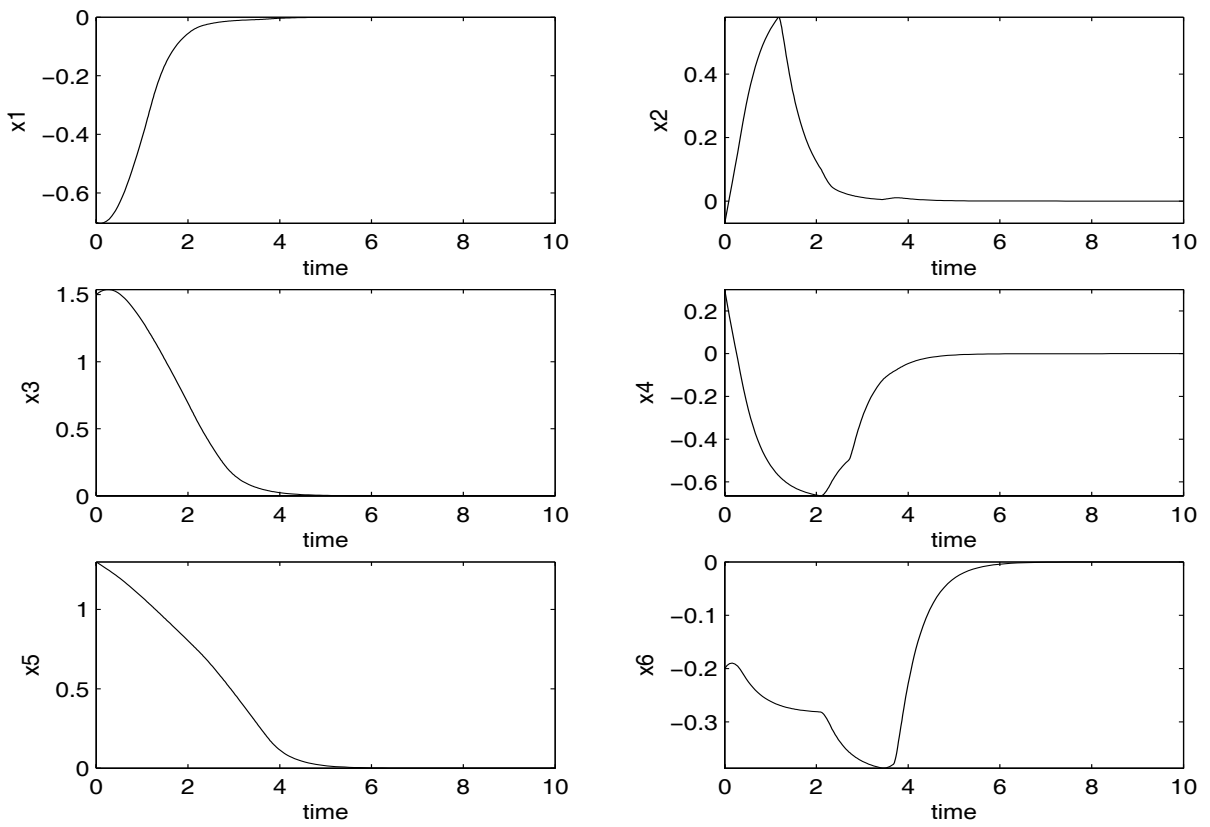
Table 2.1: Performances of passive control (designed for u_2 fail)

Condition	Normal	u_1	u_2	u_3	u_4
T_{con}	5.6269	X	5.6111	6.1549	X
$\int \mathbf{x}^T \mathbf{x} + \mathbf{u}^T \mathbf{u}$	11.1275	X	10.1268	13.4349	X
$\int \mathbf{u}^T \mathbf{u}$	2.9085	X	1.8908	5.0636	X
$\ \mathbf{u}\ _\infty$	1	X	1	1	X

Table 2.2: Performances of active control

Condition	Normal	u_1	u_2	u_3	u_4
T_{con}	9.8095	9.6085	9.8727	9.834	10.0018
$\int \mathbf{x}^T \mathbf{x} + \mathbf{u}^T \mathbf{u}$	14.2708	14.0952	14.5304	14.5536	14.6385
$\int \mathbf{u}^T \mathbf{u}$	0.3303	0.4889	0.495	0.4746	0.4849
$\ \mathbf{u}\ _\infty$	0.5608	0.5608	0.5608	0.5608	0.5608

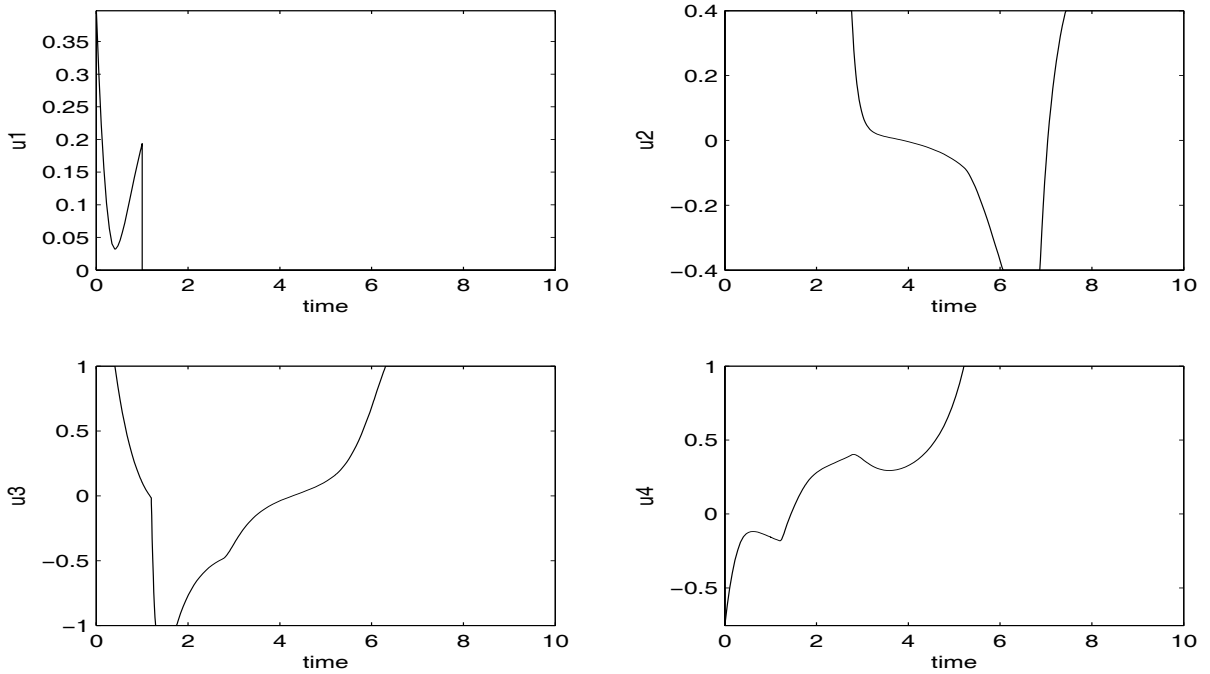
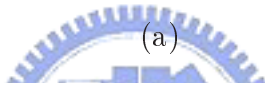
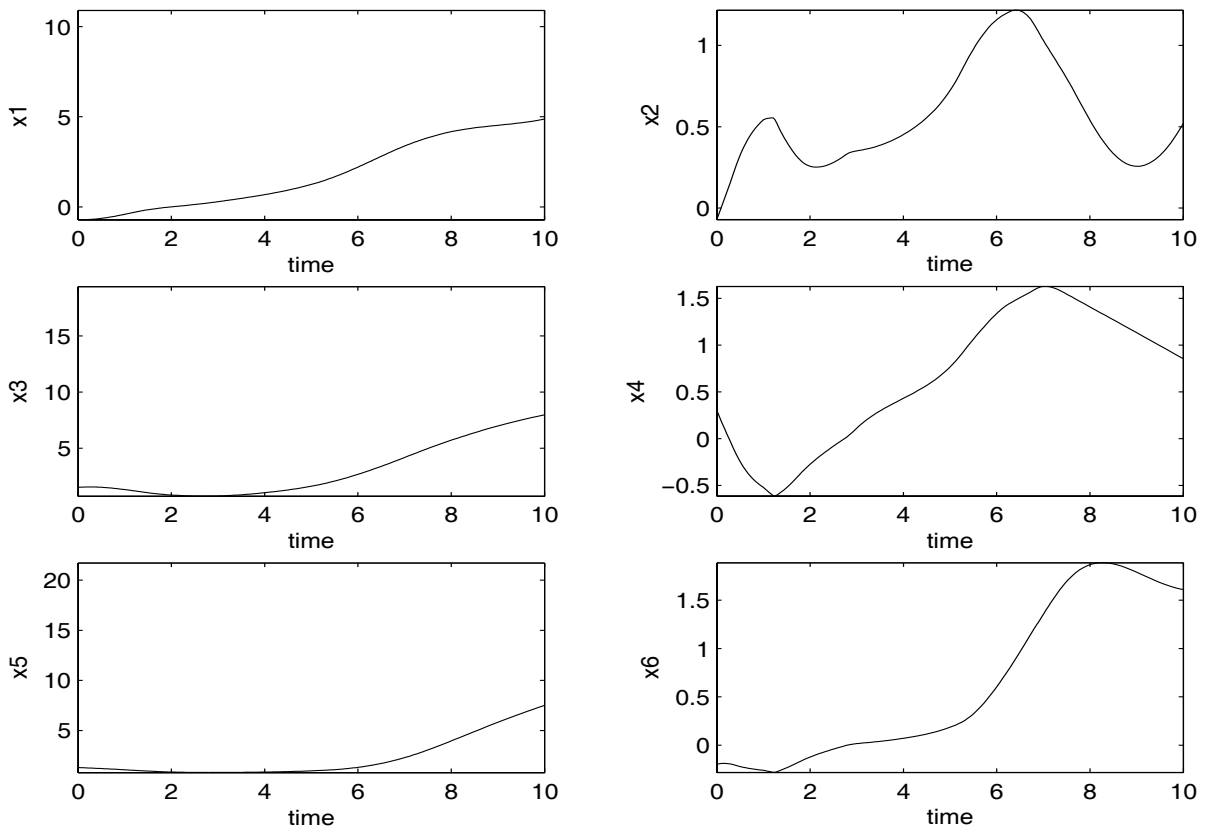




(b)

Figure 2.6: Passive control when normal operation (design for u_2 outage)

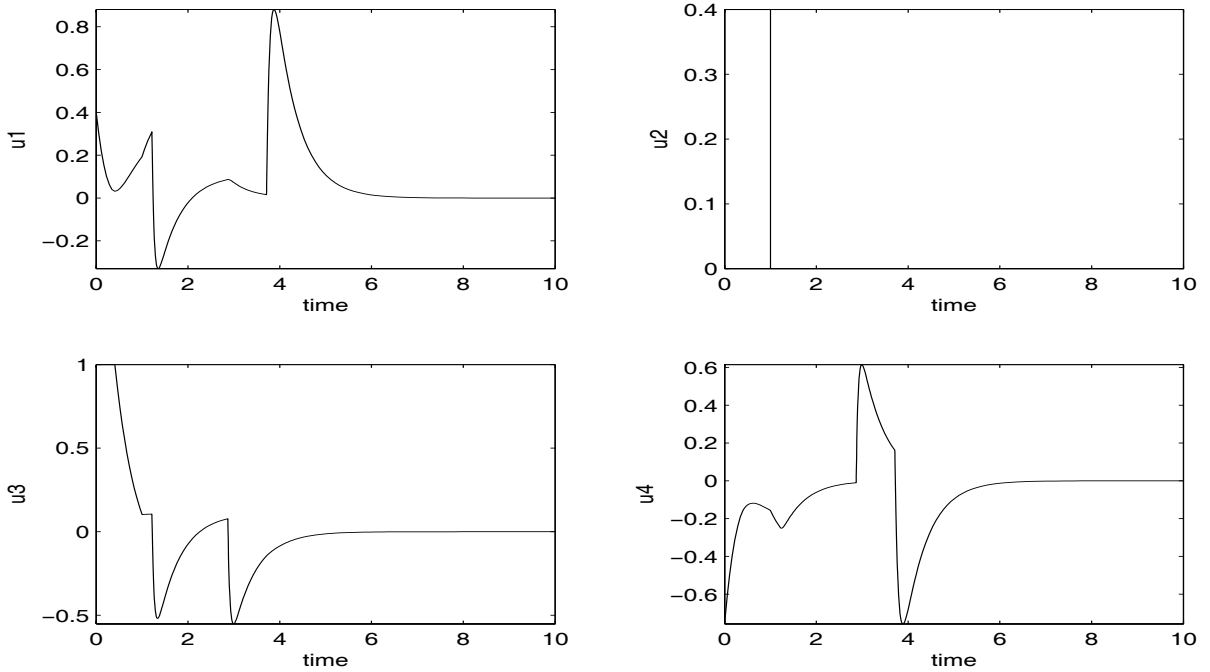
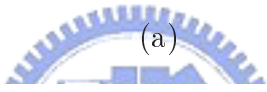
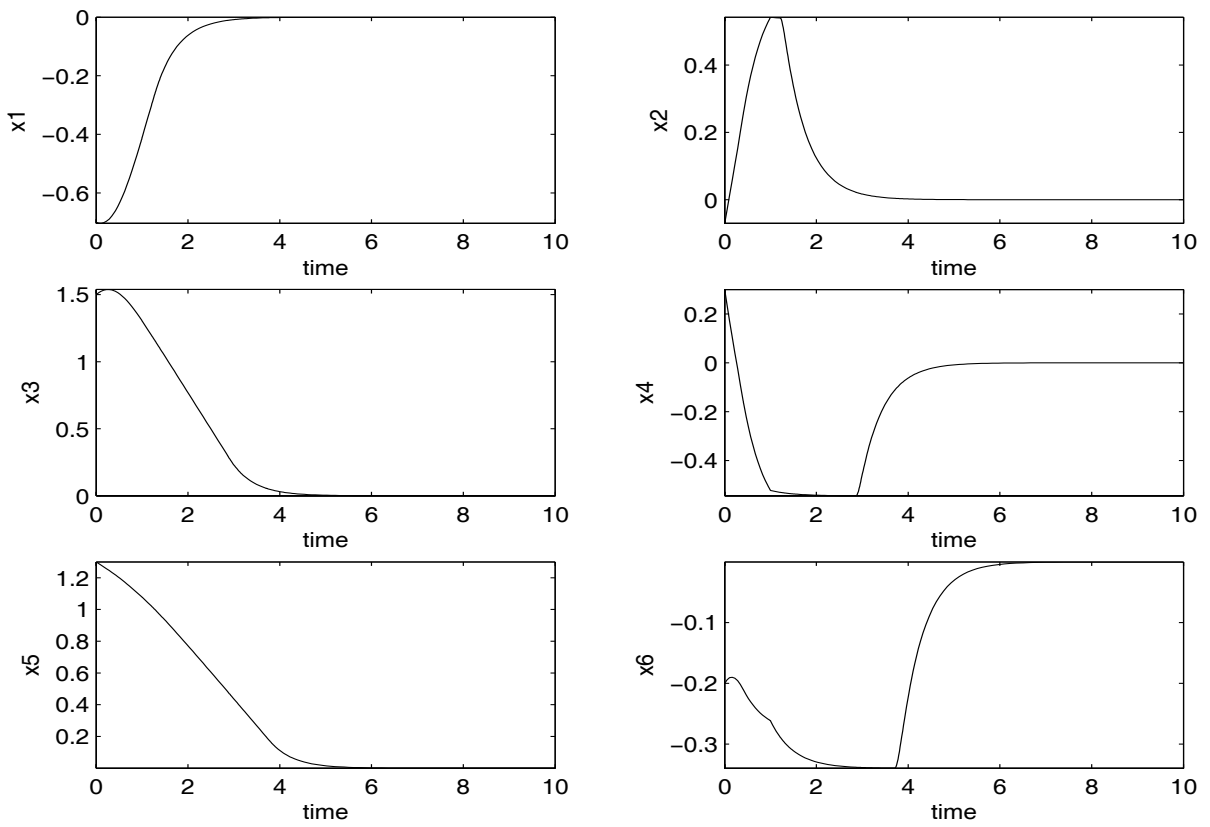
(a) states (b) input torque



(b)

Figure 2.7: Passive control when u_1 fail (design for u_2 outage)

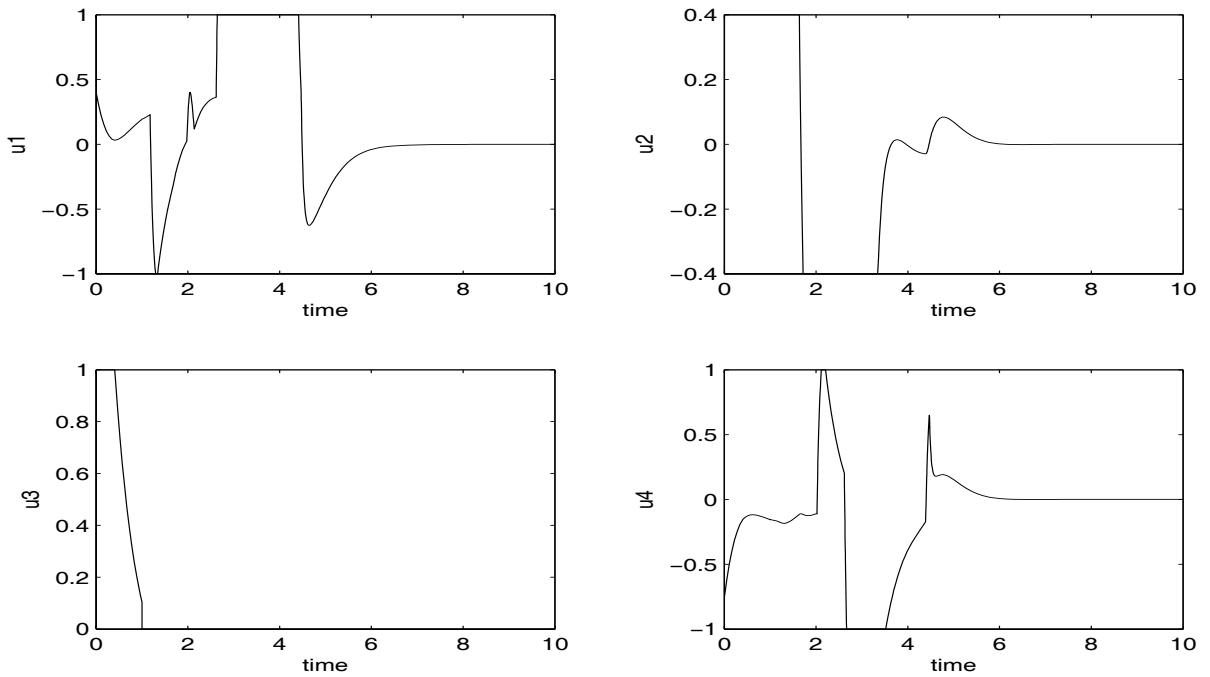
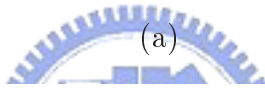
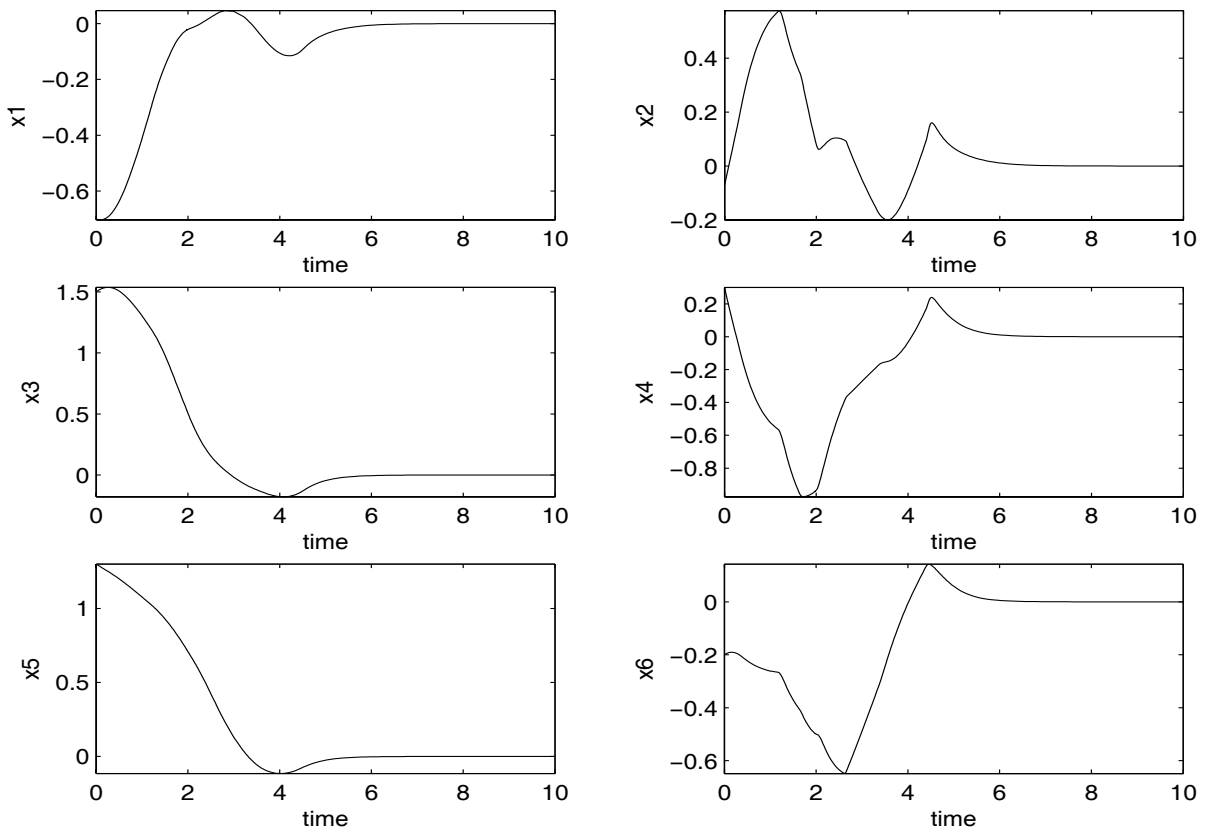
(a) states (b) input torque



(b)

Figure 2.8: Passive control when u_2 fail (design for u_2 outage)

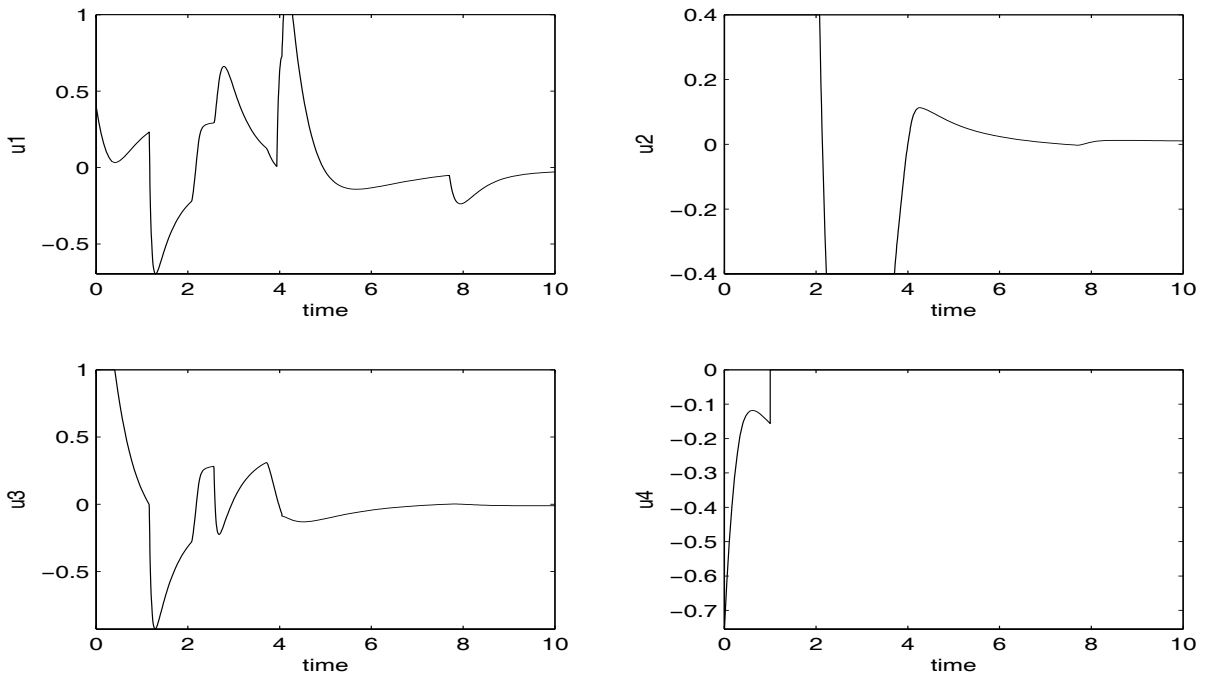
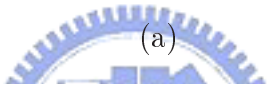
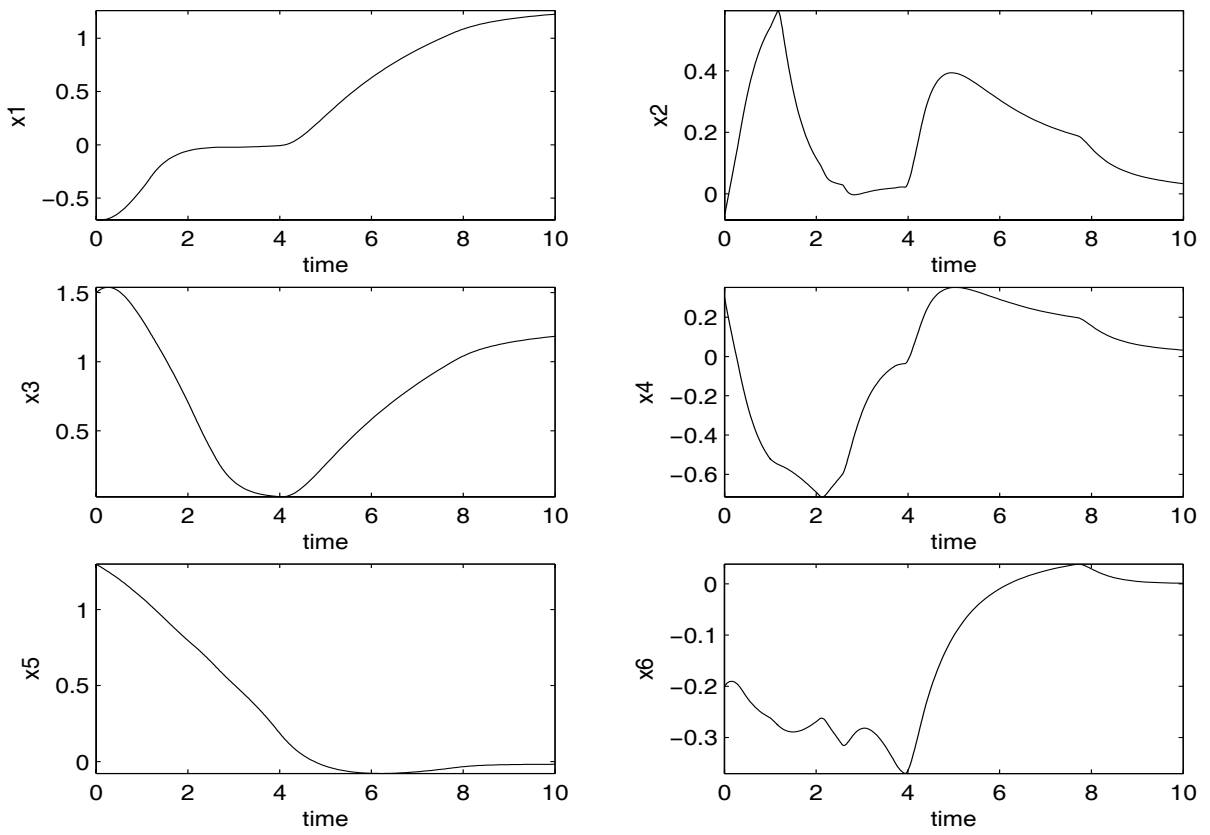
(a) states (b) input torque



(b)

Figure 2.9: Passive control when u_3 fail (design for u_2 outage)

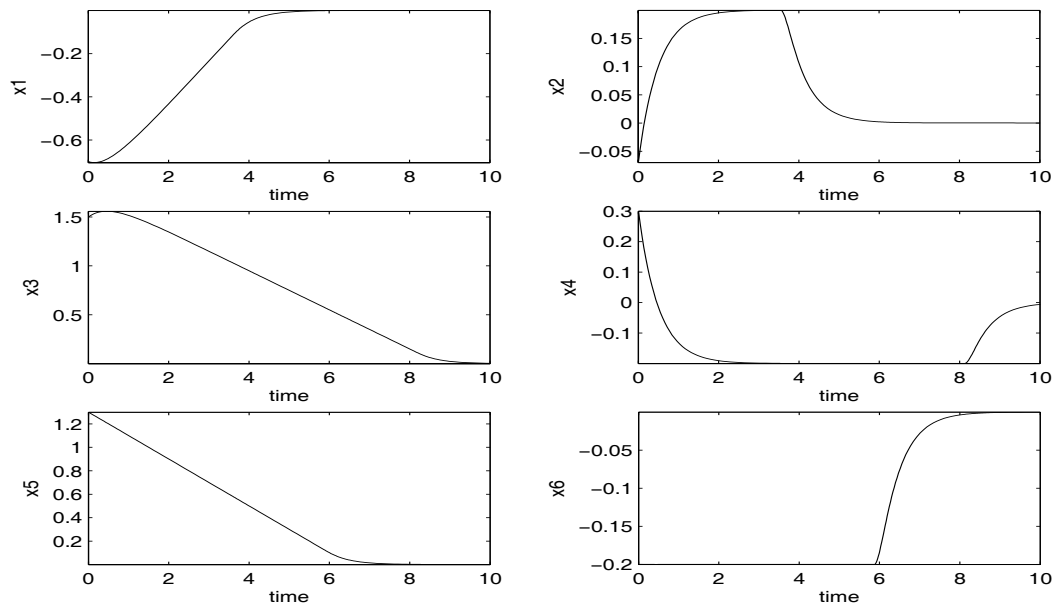
(a) states (b) input torque



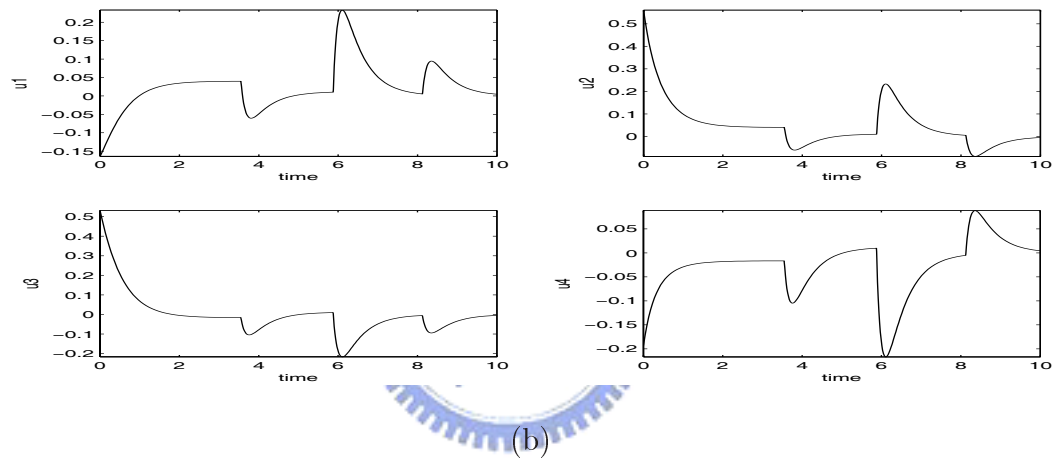
(b)

Figure 2.10: Passive control when u_4 fail (design for u_2 outage)

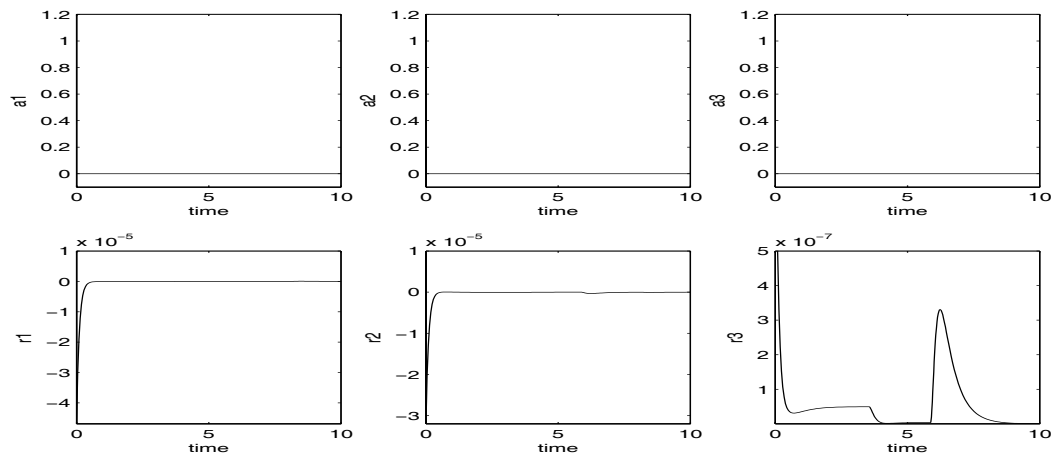
(a) states (b) input torque



(a)



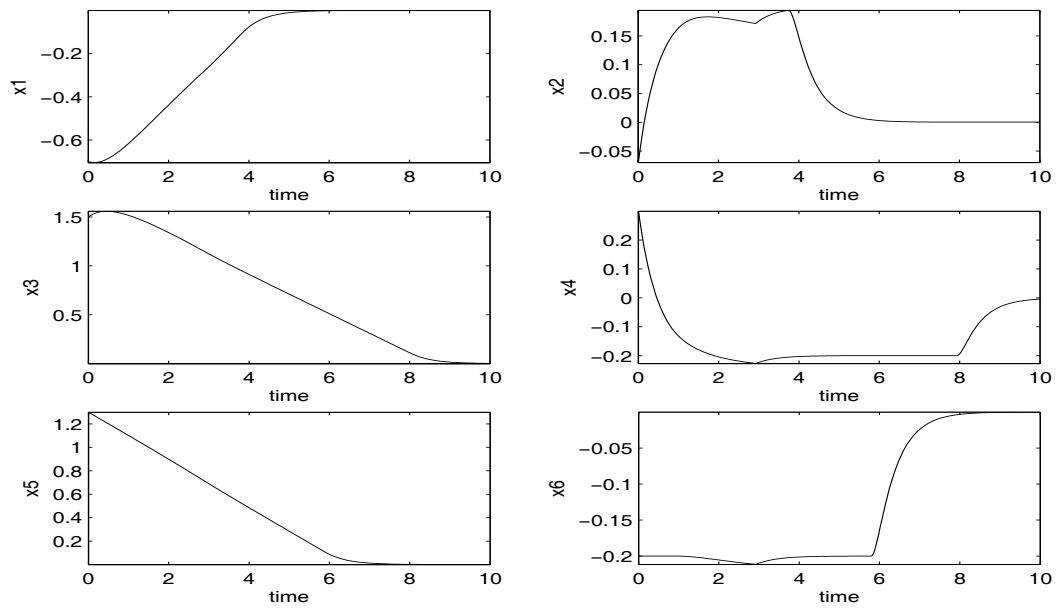
(b)



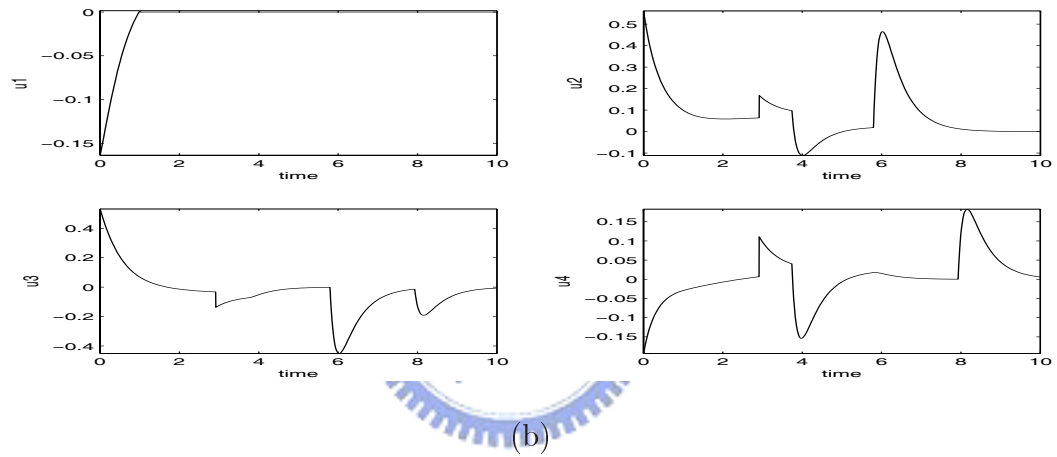
(c)

Figure 2.11: Active control when normal operation

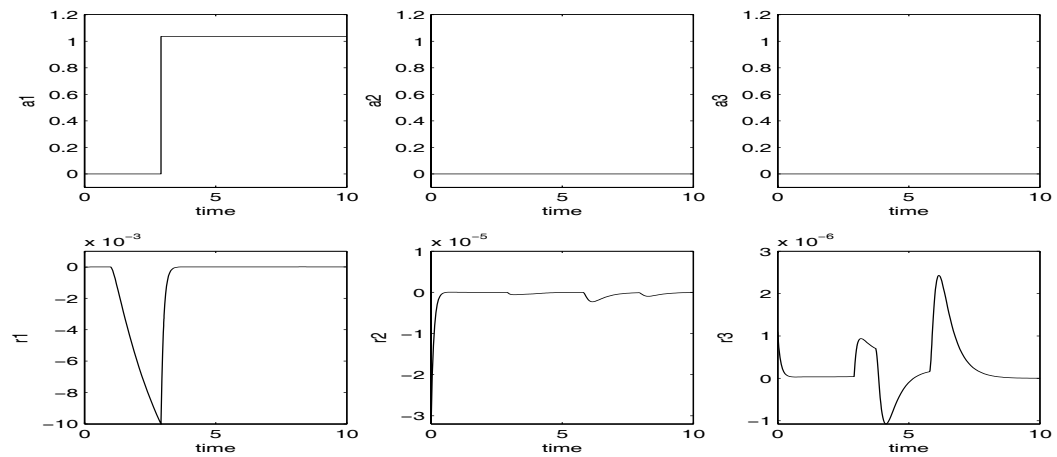
(a) states (b) input torque (c) alarms and residual



(a)



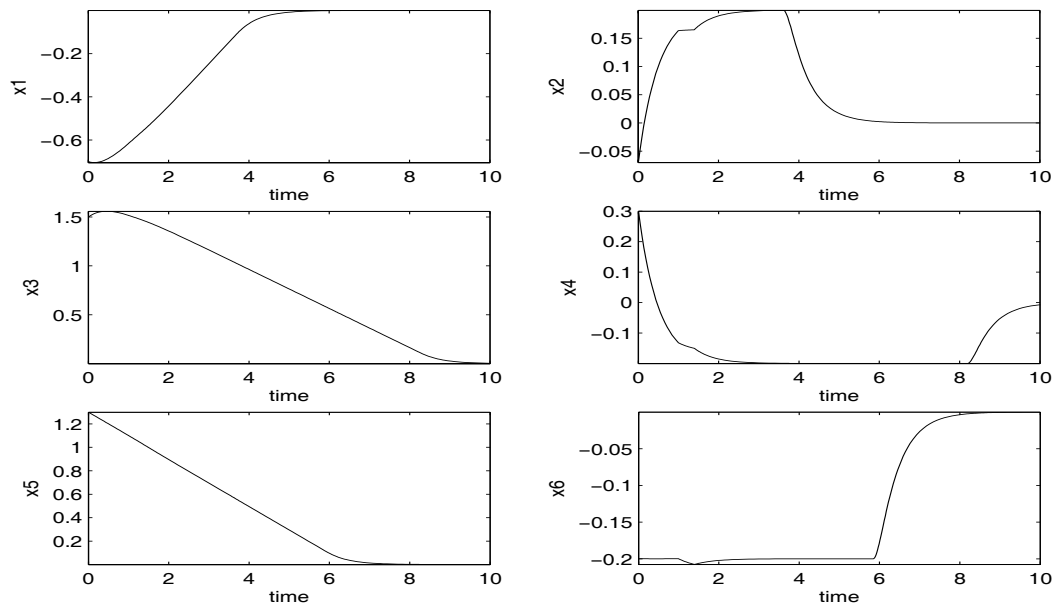
(b)



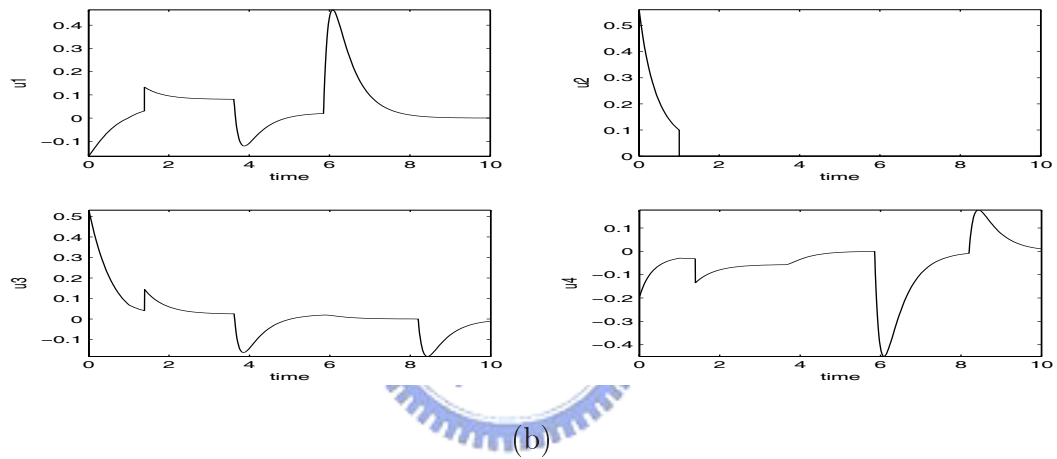
(c)

Figure 2.12: Active control when u_1 fail

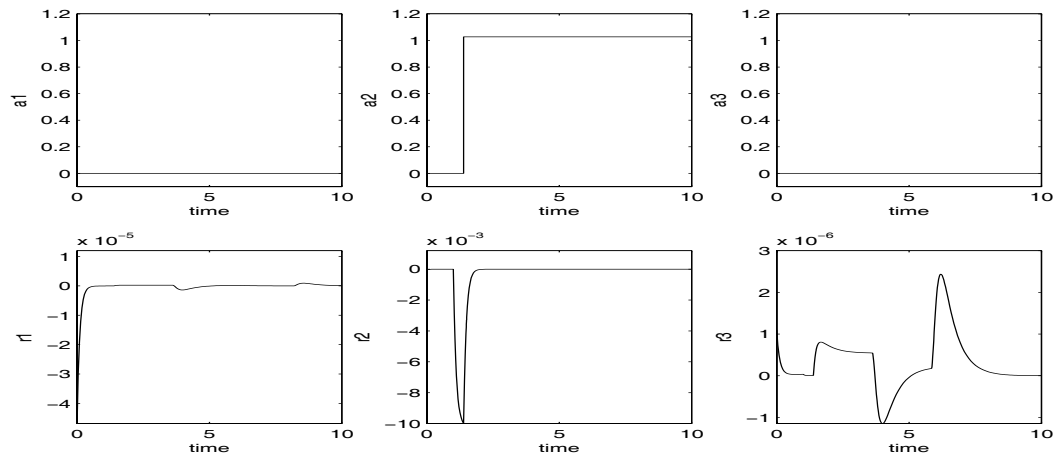
(a) states (b) input torque (c) alarms and residual



(a)



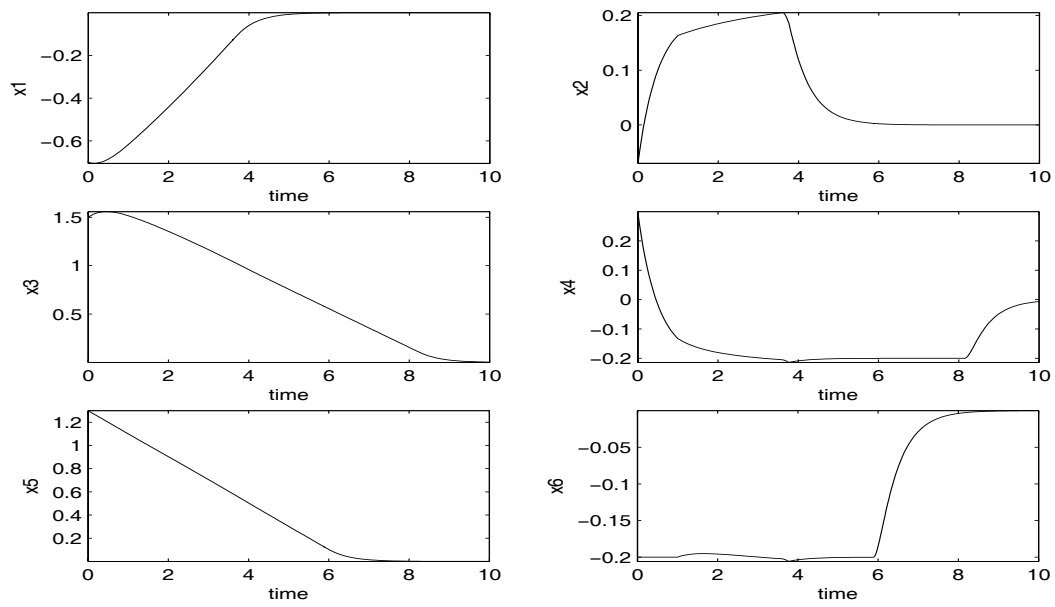
(b)



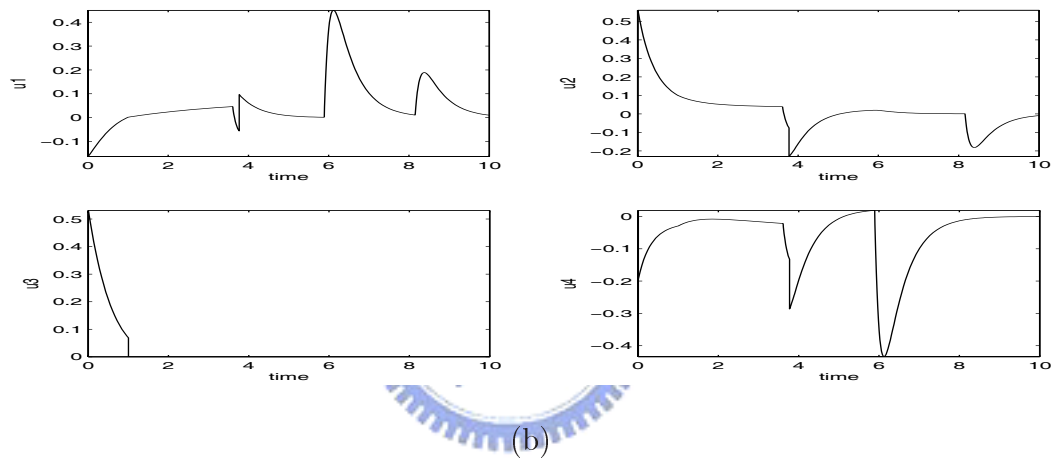
(c)

Figure 2.13: Active control when u_2 fail

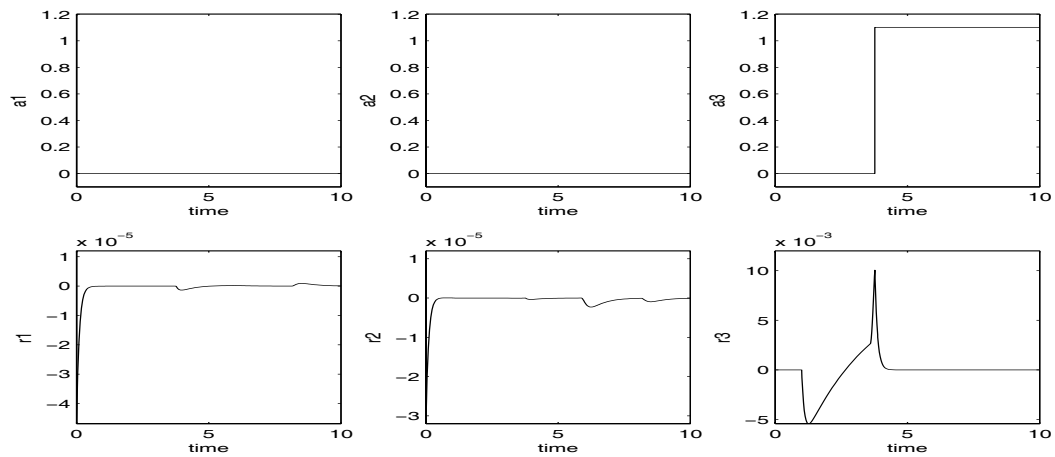
(a) states (b) input torque (c) alarms and residual



(a)



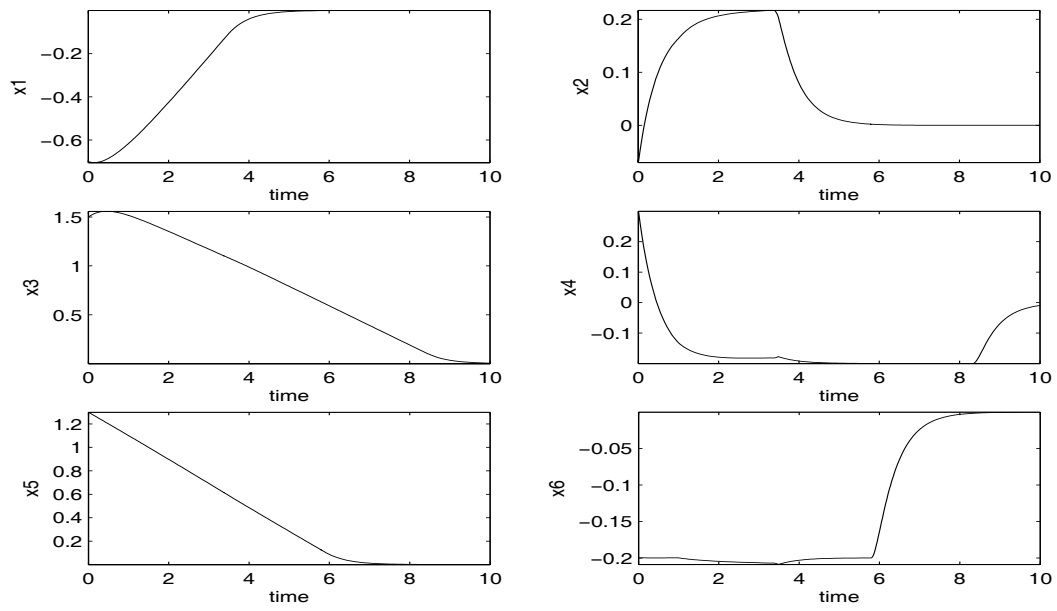
(b)



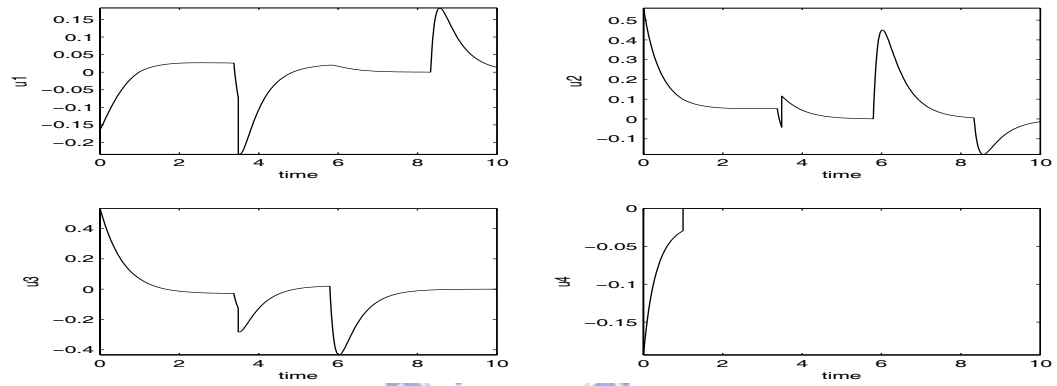
(c)

Figure 2.14: Active control when u_3 fail

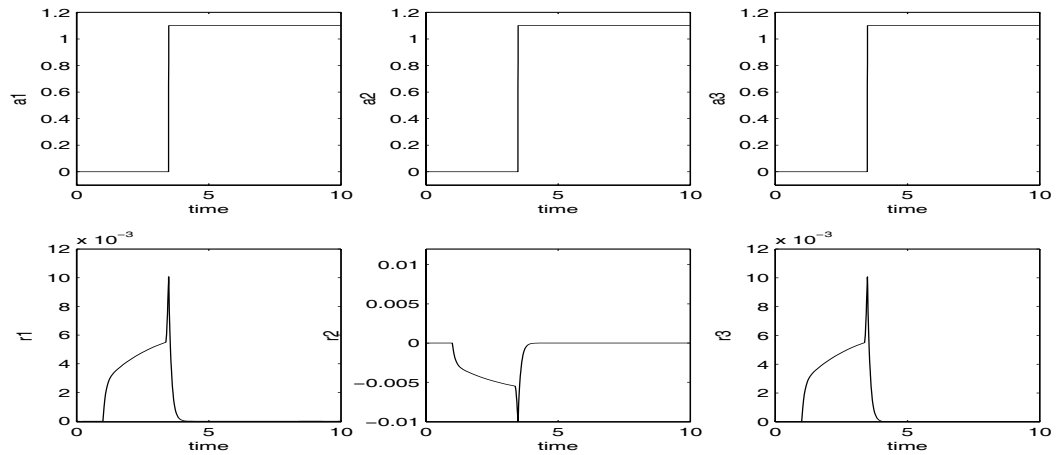
(a) states (b) input torque (c) alarms and residual



(a)



(b)



(c)

Figure 2.15: Active control when u_4 fail

(a) states (b) input torque (c) alarms and residual

CHAPTER THREE

MEASUREMENT OF CONTROLLABILITY

3.1 Introduction

The classical methods of testing controllability of a linear multivariable system involve determining whether or not a certain matrix has rank equal to the order of the system. For example, a frequently used method to test the controllability of a n -dimensional system pair (\mathbf{A}, \mathbf{B}) , where $\mathbf{A} \in \mathbb{R}^{n \times n}$ and $\mathbf{B} \in \text{real}^{n \times m}$, is to check whether or not the $n \times nm$ controllability matrix $C = [\mathbf{B} \ \mathbf{AB} \ \mathbf{A}^2\mathbf{B} \ \dots \ \mathbf{A}^{n-1}\mathbf{B}]$ has rank n (full row rank). However, these tests provide only "yes" or "not" answer for the controllability of a system, generally speaking, do not provide satisfactory one due to the finite accuracy of the computation and the parameters of a system, which are known only approximately. As a result, one may lead to wrong conclusions if such binary tests are used (e.g., one may determine a system as a controllable one but actually not, and always do not know why the system can not reach the performance as he thought). It is, therefore, useful to define controllability measure base on continuous rather than binary.

In this chapter, we are going to introduce two continuous controllability measurements, "The Distance to Uncontrollable" (see e.g., [3], [7], [10], [11], [24], [26]) and "Mobility of Eigenvalues", proposed by Tarokh [31], [33], [34]. The concept of the first one is to define an uncontrollable set, then find out the shortest distance form the original system to it. The drawback of this method is one must to determine the singular value of a polynomial matrix and minimizing a function of a complex variable, which is complicated. The manner of the second one is to determine the ability of an eigenvalue to move a very small distance to the neighborhood of its own. Both two methods have their own opinions and benefits, and we will give detailed interpretations in this chapter.

Note that, the controllability measurements in this chapter are been developed upon linear system, and the associated research had not been extend to nonlinear system yet, therefore, only the linear system will be considered here. About the issues of nonlinear system, we leave them for the further research.

3.2 Defects of Classical Controllability Measurement

From linear system theory, we know that if a system is controllable, then we can transfer it's states to any where at any time as we desired. One may wonder what is the difference between an easier controllable system and a harder one? Before discussing the new methods for continuous controllability measurements, we take an example to show why binary test is not sufficient.

There are many methods to determine the contollability of a linear system model $\dot{x} = \mathbf{A}x + \mathbf{B}u$, where $\mathbf{A} \in \mathbb{R}^{n \times n}$, $x \in \mathbb{R}^n$, $\mathbf{B} \in \mathbb{R}^{n \times m}$ and $u \in \mathbb{R}^m$. We list five of them which are equivalent as follows (see e.g., [5]).

1. The n -dimensional pair (\mathbf{A}, \mathbf{B}) is controllable.
2. The $n \times n$ matrix

$$\mathbf{W}_c(t) = \int_0^t e^{\mathbf{A}\tau} \mathbf{B} \mathbf{B}^T e^{\mathbf{A}\tau} d\tau = \int_0^t e^{\mathbf{A}(t-\tau)} \mathbf{B} \mathbf{B}^T e^{\mathbf{A}(t-\tau)} d\tau \quad (3.1)$$

is nonsingular for any $t > 0$.

3. The $n \times nm$ controllability matrix

$$\mathbf{C} = [\mathbf{B} \quad \mathbf{A}\mathbf{B} \quad \mathbf{A}^2\mathbf{B} \quad \dots \quad \mathbf{A}^{n-1}\mathbf{B}] \quad (3.2)$$

has rank n (full row rank).

4. The $n \times (n + m)$ matrix $[\mathbf{A} - \lambda\mathbf{I}, \mathbf{B}]$ has full row rank at every eigenvalue, λ , of \mathbf{A} .

$$(3.3)$$

5. If all eigenvalues of \mathbf{A} have negative real parts, then the unique solution of

$$\mathbf{A}\mathbf{W}_c + \mathbf{W}_c\mathbf{A}^T = -\mathbf{B}\mathbf{B}^T \quad (3.4)$$

is positive define. The solution is

$$\mathbf{W}_c = \int_0^{\infty} e^{\mathbf{A}\tau} \mathbf{B} \mathbf{B}^T e^{\mathbf{A}^T \tau} d\tau \quad (3.5)$$

3.2.1 Controllability Analysis of Spacecraft

Now we employ the checking condition (3.2) to determine controllability of the spacecraft model. To employ the result, we linearize the nonlinear state equation (2.48) with equilibrium point being the origin. It yields

$$\mathbf{A} = \begin{pmatrix} 0 & 1 & 0 & 0 & 0 & 0 \\ -2a_1 & 0 & 0 & 0 & 0 & a_2 \\ 0 & 0 & 0 & 1 & 0 & 0 \\ 0 & 0 & 0 & 0 & 0 & 0 \\ 0 & 0 & 0 & 0 & 0 & 1 \\ 0 & -a_2 & 0 & 0 & a_1 & 0 \end{pmatrix} \quad (3.6)$$

$$\mathbf{B} = \begin{pmatrix} 0 & 0 & 0 & 0 \\ 0.67 & 0.67 & 0.67 & 0.67 \\ 0 & 0 & 0 & 0 \\ 0.69 & -0.69 & -0.69 & 0.69 \\ 0 & 0 & 0 & 0 \\ 0.28 & 0.28 & -0.28 & -0.28 \end{pmatrix} \quad (3.7)$$

where $a_1 = \omega_0^2(I_y - I_x)/I_z$, $a_2 = \omega_0 I_y/I_x$. It is easy to show that the characteristic polynomial of \mathbf{A} has the form

$$\lambda^2 \cdot [\lambda^4 + (a_1 + a_2^2)\lambda^2 - 2a_1^2] = 0$$

Thus, the eigenvalues of matrix \mathbf{A} are $(0, 0, \pm\mu_1, \pm j\mu_2)$, where $\mu_1 = \sqrt{\frac{\sqrt{(a_1+a_2^2)^2+8a_1^2}-(a_1+a_2^2)}{2}}$ and $\mu_2 = \sqrt{\frac{\sqrt{(a_1+a_2^2)^2+8a_1^2}+(a_1+a_2^2)}{2}}$. Because μ_1 and μ_2 are positive, it is clear that the zero input system is unstable.

Next, we analyze the controllability. By selecting the system parameters as $I_x = I_z = 2000N \cdot m \cdot s^2$ and $I_y = 400N \cdot m \cdot s^2$, which means that the inertia of system is symmetric with y axis and $\omega_0 = 1.0312 \times 10^{-3} rad/s$, then we have $a_1 = -8.507 \times 10^{-7}$ and $a_2 = 2.6024 \times 10^{-4}$. To proceed the analysis, we define the symbols to represent faulty system $(\mathbf{A}, \mathbf{B}_f)$ under different outage cases as below:

B : normal case (i.e., all actuators are in normal operation).

B_i : case for single (i -th) actuator fails, for $i = 1, 2, 3, 4$.

B_{ij} : case for double (i -th and j -th) actuators fail, for $i, j = 1, 2, 3, 4$, $i \neq j$.

Under these notations, the controllability matrix of equation (3.2) becomes

$$C_{B_f} = [B_f \quad \mathbf{A}B_f \quad \mathbf{A}^2B_f \quad \cdots \quad \mathbf{A}^5B_f] \quad (3.8)$$

By calculation, the controllability matrices with different actuator outage are listed below (due to the limitation of the printed page, only the first six linearly independent columns for each case are listed).

when $B_f = B$,

$$C_B = \begin{pmatrix} 0 & 0 & 0 & 0.67 & 0.67 & 0.67 \\ 0.67 & 0.67 & 0.67 & 5.77 \times 10^{-5} & 5.77 \times 10^{-5} & -5.77 \times 10^{-5} \\ 0 & 0 & 0 & 0.69 & -0.69 & -0.69 \\ 0.69 & -0.69 & -0.69 & 0 & 0 & 0 \\ 0 & 0 & 0 & 0.28 & 0.28 & -0.28 \\ 0.28 & 0.28 & -0.28 & -1.4 \times 10^{-4} & -1.4 \times 10^{-4} & -1.4 \times 10^{-4} \end{pmatrix}$$

when $B_f = B_1$,

$$C_{B_1} = \begin{pmatrix} 0 & 0 & 0 & 0.67 & 0.67 & 0.67 \\ 0.67 & 0.67 & 0.67 & 5.77 \times 10^{-5} & -5.77 \times 10^{-5} & -5.77 \times 10^{-5} \\ 0 & 0 & 0 & -0.69 & -0.69 & 0.69 \\ -0.69 & -0.69 & 0.69 & 0 & 0 & 0 \\ 0 & 0 & 0 & 0.28 & -0.28 & -0.28 \\ 0.28 & -0.28 & -0.28 & -1.4 \times 10^{-4} & -1.4 \times 10^{-4} & -1.4 \times 10^{-4} \end{pmatrix}$$

when $B_f = B_2$,

$$C_{B_2} = \begin{pmatrix} 0 & 0 & 0 & 0.67 & 0.67 & 0.67 \\ 0.67 & 0.67 & 0.67 & 5.77 \times 10^{-5} & -5.77 \times 10^{-5} & -5.77 \times 10^{-5} \\ 0 & 0 & 0 & 0.69 & -0.69 & 0.69 \\ 0.69 & -0.69 & 0.69 & 0 & 0 & 0 \\ 0 & 0 & 0 & 0.28 & -0.28 & -0.28 \\ 0.28 & -0.28 & -0.28 & -1.4 \times 10^{-4} & -1.4 \times 10^{-4} & -1.4 \times 10^{-4} \end{pmatrix}$$

when $B_f = B_3$,

$$C_{B_3} = \begin{pmatrix} 0 & 0 & 0 & 0.67 & 0.67 & 0.67 \\ 0.67 & 0.67 & 0.67 & 5.77 \times 10^{-5} & 5.77 \times 10^{-5} & -5.77 \times 10^{-5} \\ 0 & 0 & 0 & 0.69 & -0.69 & 0.69 \\ 0.69 & -0.69 & 0.69 & 0 & 0 & 0 \\ 0 & 0 & 0 & 0.28 & 0.28 & -0.28 \\ 0.28 & 0.28 & -0.28 & -1.4 \times 10^{-4} & -1.4 \times 10^{-4} & -1.4 \times 10^{-4} \end{pmatrix}$$

when $B_f = B_4$,

$$C_{B_4} = \begin{pmatrix} 0 & 0 & 0 & 0.67 & 0.67 & 0.67 \\ 0.67 & 0.67 & 0.67 & 5.77 \times 10^{-5} & 5.77 \times 10^{-5} & -5.77 \times 10^{-5} \\ 0 & 0 & 0 & 0.69 & -0.69 & -0.69 \\ 0.69 & -0.69 & -0.69 & 0 & 0 & 0 \\ 0 & 0 & 0 & 0.28 & 0.28 & -0.28 \\ 0.28 & 0.28 & -0.28 & -1.4 \times 10^{-4} & -1.4 \times 10^{-4} & -1.4 \times 10^{-4} \end{pmatrix}$$

when $B_f = B_{12}$,

$$C_{B_{12}} = \begin{pmatrix} 0 & 0 & 0.67 & 0.67 & -5.77 \times 10^{-5} & 1.11 \times 10^{-6} \\ 0.67 & 0.67 & -5.77 \times 10^{-5} & -5.77 \times 10^{-5} & 1.11 \times 10^{-6} & -4.67 \times 10^{-11} \\ 0 & 0 & -0.69 & 0.69 & 0 & 0 \\ -0.69 & 0.69 & 0 & 0 & 0 & 0 \\ 0 & 0 & -0.28 & -0.28 & -1.4 \times 10^{-4} & 2.50 \times 10^{-7} \\ -0.28 & -0.28 & -1.4 \times 10^{-4} & -1.4 \times 10^{-4} & 2.50 \times 10^{-7} & -1.12 \times 10^{-10} \end{pmatrix}$$

when $B_f = B_{13}$,

$$C_{B_{13}} = \begin{pmatrix} 0 & 0 & 0.67 & 0.67 & 5.77 \times 10^{-5} & -5.77 \times 10^{-5} \\ 0.67 & 0.67 & 5.77 \times 10^{-5} & -5.77 \times 10^{-5} & 1.11 \times 10^{-6} & 1.11 \times 10^{-6} \\ 0 & 0 & -0.69 & 0.69 & 0 & 0 \\ -0.69 & 0.69 & 0 & 0 & 0 & 0 \\ 0 & 0 & 0.28 & -0.28 & -1.4 \times 10^{-4} & -1.4 \times 10^{-4} \\ 0.28 & -0.28 & -1.4 \times 10^{-4} & -1.4 \times 10^{-4} & -2.50 \times 10^{-7} & 2.50 \times 10^{-7} \end{pmatrix}$$

when $B_f = B_{14}$,

$$C_{B_{14}} = \begin{pmatrix} 0 & 0 & 0.67 & 0.67 & 5.77 \times 10^{-5} & -5.77 \times 10^{-5} \\ 0.67 & 0.67 & 5.77 \times 10^{-5} & -5.77 \times 10^{-5} & 1.11 \times 10^{-6} & 1.11 \times 10^{-6} \\ 0 & 0 & -0.69 & -0.69 & 0 & 0 \\ -0.69 & -0.69 & 0 & 0 & 0 & 0 \\ 0 & 0 & 0.28 & -0.28 & -1.4 \times 10^{-4} & -1.4 \times 10^{-4} \\ 0.28 & -0.28 & -1.4 \times 10^{-4} & -1.4 \times 10^{-4} & -2.50 \times 10^{-7} & 2.50 \times 10^{-7} \end{pmatrix}$$

when $B_f = B_{23}$,

$$C_{B_{23}} = \begin{pmatrix} 0 & 0 & 0.67 & 0.67 & 5.77 \times 10^{-5} & -5.77 \times 10^{-5} \\ 0.67 & 0.67 & 5.77 \times 10^{-5} & -5.77 \times 10^{-5} & 1.11 \times 10^{-6} & 1.11 \times 10^{-6} \\ 0 & 0 & 0.69 & 0.69 & 0 & 0 \\ 0.69 & 0.69 & 0 & 0 & 0 & 0 \\ 0 & 0 & 0.28 & -0.28 & -1.4 \times 10^{-4} & -1.4 \times 10^{-4} \\ 0.28 & -0.28 & -1.4 \times 10^{-4} & -1.4 \times 10^{-4} & -2.50 \times 10^{-7} & 2.50 \times 10^{-7} \end{pmatrix}$$

when $B_f = B_{24}$,

$$C_{B_{24}} = \begin{pmatrix} 0 & 0 & 0.67 & 0.67 & 5.77 \times 10^{-5} & -5.77 \times 10^{-5} \\ 0.67 & 0.67 & 5.77 \times 10^{-5} & -5.77 \times 10^{-5} & 1.11 \times 10^{-6} & 1.11 \times 10^{-6} \\ 0 & 0 & 0.69 & -0.69 & 0 & 0 \\ 0.69 & -0.69 & 0 & 0 & 0 & 0 \\ 0 & 0 & 0.28 & -0.28 & -1.4 \times 10^{-4} & -1.4 \times 10^{-4} \\ 0.28 & -0.28 & -1.4 \times 10^{-4} & -1.4 \times 10^{-4} & -2.50 \times 10^{-7} & 2.50 \times 10^{-7} \end{pmatrix}$$

when $B_f = B_{34}$,

$$C_{B_{34}} = \begin{pmatrix} 0 & 0 & 0.67 & 0.67 & 5.77 \times 10^{-5} & 1.11 \times 10^{-6} \\ 0.67 & 0.67 & 5.77 \times 10^{-5} & 5.77 \times 10^{-5} & 1.11 \times 10^{-6} & 4.67 \times 10^{-11} \\ 0 & 0 & 0.69 & -0.69 & 0 & 0 \\ 0.69 & -0.69 & 0 & 0 & 0 & 0 \\ 0 & 0 & 0.28 & 0.28 & -1.4 \times 10^{-4} & -2.50 \times 10^{-7} \\ 0.28 & 0.28 & -1.4 \times 10^{-4} & -1.4 \times 10^{-4} & -2.50 \times 10^{-7} & -1.12 \times 10^{-10} \end{pmatrix}$$

It is noted that $\text{rank}(C_B) = \text{rank}(C_{B_1}) = \text{rank}(C_{B_2}) = \dots = \text{rank}(C_{B_{34}}) = 6$, which implies that the system are always controllable no matter any one or two actuators experience faults.

3.2.2 Energy Required to Transfer States

From last section, we see an interesting result: no matter one or two actuators fail, the system is still controllable. Theoretically, we can control the states to any locations whatever cases discussed above, but how about in practical? Here, we begin from the viewpoint of energy. Consider a linear time-invariant control system

$$\dot{x}(t) = \mathbf{A}x(t) + \mathbf{B}u(t) \quad (3.9)$$

and associated controllability Gramian

$$\mathbf{W}_c(t) = \int_0^t e^{\mathbf{A}\tau} \mathbf{B} \mathbf{B}^T e^{\mathbf{A}\tau} d\tau \quad (3.10)$$

if the system is controllable, we know that for any initial state $x(0) = x_0$ at time $t = 0$ and any final state $x(t_1) = x_1$ at time $t = t_1$, the input

$$u(t) = -\mathbf{B}^T e^{\mathbf{A}^T(t_1-t)} \mathbf{W}_c^{-1}(t_1) [e^{\mathbf{A}t_1} x_0 - x_1] \quad (3.11)$$

will transfer x_0 at time $t = 0$ to x_1 at time t_1 . The associated required energy is

$$E = \int_0^{t_1} u^T(t)u(t)dt = [e^{\mathbf{A}t_1}x_0 - x_1]^T \mathbf{W}_c^{-1}(t_1)[e^{\mathbf{A}t_1}x_0 - x_1] \quad (3.12)$$

Now, we use this result to proceed a test. To transfer the spacecraft states from $x(0) = (-0.7, -0.07, 1.5, 0.3, 1.3, -0.2)^T$ at $t = 0$ to $x(t_1) = (\mathbf{0})$ at $t_1 = 100$ second, the energy required to achieve the task is listed in Table 3.1, where each condition is considered involved.

Table 3.1: Energy required to transfer states

Condition	B	B_1	B_2	B_3	B_4
Energy	6.50×10^{-3}	7.40×10^{-3}	2.17×10^{-2}	6.60×10^{-3}	1.63×10^{-2}
Condition	B_{12}	B_{13}	B_{14}		
Energy	3.69×10^6	3.90×10^3	2.81×10^3		
Condition	B_{23}	B_{24}	B_{34}		
Energy	7.94×10^3	6.61×10^4	9.56×10^5		

From this table we can see that the energy required to transfer the states is about the level of 10^{-2} or 10^{-3} when normal operation or only one actuator is fail, while it up to the level of 10^6 at most when two actuators work abnormal, even the smallest ratio between them ($E = 2.17 \times 10^{-2}$ of faulty condition B_2 and $E = 2.81 \times 10^3$ of faulty condition B_{14}) is approximately 1.3×10^5 . Of course, it is no doubt that those cases when two actuators fail are controllable, we can still achieve the task, nevertheless we need more energy, and not only a few (at least 1.3×10^5 times larger).

Spacecraft is an expensive equipment, and most of it's working life depends upon the remainder energy it has, the example we show above may tell us that it is not worth to executive such a mission while any two actuators are fail. However, the unperfection is that the situations we discussed above are only case by case, that is, to transfer a specified state to another one. Therefore, we are going to give more general descriptions about the controllability in the following sections.

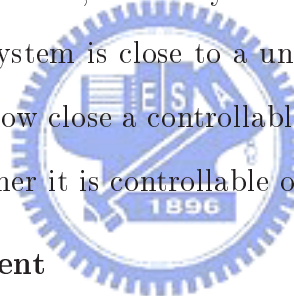
3.3 Distance to Uncontrollable

3.3.1 Introduction

The concepts of controllability [6], [9], [10] is a generic property. Since to determine if a system is controllable depends upon whether a certain matrix has full rank, it is clear that an uncontrollable system can arbitrary close to a controllable one as long as it is still stay uncontrollable. To illustrate this, consider a well-known example (Eising 1984):

$$\mathbf{A} = \begin{pmatrix} -1 & -1 & \cdot & \cdot & \cdot & -1 & -1 \\ 1 & -1 & & & & & -1 \\ & 1 & \cdot & & & & \cdot \\ & & \cdot & \cdot & & & \cdot \\ & & & \cdot & \cdot & & \cdot \\ \mathbf{0} & & & \cdot & -1 & -1 & \\ & & & & 1 & 1 & \end{pmatrix}, \quad \mathbf{B} = \begin{pmatrix} 1 \\ 0 \\ \cdot \\ \cdot \\ \cdot \\ \cdot \\ 0 \end{pmatrix}$$

After calculation, we get the pair (\mathbf{A}, \mathbf{B}) is controllable. However, if we add $(-2^{1-n}, -2^{1-n}, \dots, -2^{1-n})$ to the last row of (\mathbf{A}, \mathbf{B}) , we obtain an uncontrollable system. Here we regard the term 2^{1-n} as perturbation, obviously it is small when n is large, which implies that the original controllable system is close to a uncontrollable one. Consequently, it is more important to determine how close a controllable system is to an uncontrollable one, rather than to determine whether it is controllable only.



3.3.2 Distance Measurement

For this purpose, we introduce **a measure of the distance to uncontrollable** (Chris C. Paige(1981) [26]), denoted by $\mu(\mathbf{A}, \mathbf{B})$ as shown in Figure 3.1, which is

Definition 3.1 $\mu(\mathbf{A}, \mathbf{B}) \equiv \min \{ \|\Delta\mathbf{A}, \Delta\mathbf{B}\|_2 \text{ such that the system}$
 $\text{defined by } (\mathbf{A} + \Delta\mathbf{A}, \mathbf{B} + \Delta\mathbf{B}) \text{ is uncontrollable.} \}$

where $\|\cdot\|_2$ is 2-norm, and $\Delta\mathbf{A}$ and $\Delta\mathbf{B}$ are allowable perturbations over a field F. The quantity $\mu(\mathbf{A}, \mathbf{B})$ gives us a measure of the distance between a controllable pair (\mathbf{A}, \mathbf{B}) and a nearest uncontrollable one, which implies that if the distance is small (large), then the original controllable system is close to (far from) an uncontrollable system. According the linear algebra theory, the distance $\mu(\mathbf{A}, \mathbf{B})$ can be defined as in Theorem 3.1. ■

Theorem 3.1 [6] Singular Value Characterization to Distance to Uncontrollable

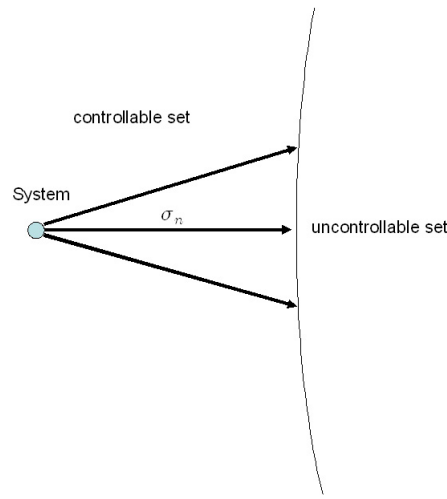


Figure 3.1: Distance to uncontrollable

$\mu(\mathbf{A}, \mathbf{B}) = \sigma_n = \sigma_{\min}[\mathbf{A} - sI, \mathbf{B}]$, where σ_n is the smallest singular value of matrix $[\mathbf{A} - sI, \mathbf{B}]$ and s runs over all complex numbers.

(3.13)

Proof: Suppose that $(\mathbf{A} + \Delta\mathbf{A}, \mathbf{B} + \Delta\mathbf{B})$ is an uncontrollable pair, according to checking condition (3.3), we have

$$\text{rank}(\mathbf{A} + \Delta\mathbf{A} - sI, \mathbf{B} + \Delta\mathbf{B}) < n, \text{ for some } s \in \mathbb{C} \quad (3.14)$$

since the smallest distance make rank $[\mathbf{A} - sI, \mathbf{B}]$ less n is $\sigma_{\min}[\mathbf{A} - sI, \mathbf{B}]$, we have

$$\sigma_{\min}[\mathbf{A} - sI, \mathbf{B}] \leq \|\Delta\mathbf{A}, \Delta\mathbf{B}\|_2 \quad (3.15)$$

and the equality holds if

$$[\Delta\mathbf{A}, \Delta\mathbf{B}] = -\sigma_n u_n v_n^* \quad (3.16)$$

where σ_n is the smallest singular value of $[\mathbf{A} - sI, \mathbf{B}]$, and u_n and v_n^* are the corresponding left and right singular vectors of σ_n , respectively. ■

The proof of Theorem 3.1 is a well-known result utilizes singular value decomposition (SVD). Since it is the most important concept here, we give a short interpretation for it. Assume A is an $m \times n$ matrix with $m \geq n$ (The assumption is made to illustrate equation (3.17), all the result still hold if $m \leq n$), then factor A into a product $U \Sigma V^*$, where U is

an $m \times m$ orthogonal matrix, V is an $n \times n$ orthogonal matrix, and Σ is an $m \times n$ matrix whose off diagonal elements are all 0's and diagonal entries satisfy

$$\sigma_1 \geq \sigma_2 \geq \cdots \geq \sigma_n \geq 0 \quad (3.17)$$

the σ_i 's are unique and are called *singular value* of A , that is, $A = U \Sigma V^*$ be the SVD of A . Let $\text{rank}(A) = n > 1$, define $A_k = U \Sigma_k V^*$, $\text{rank}(A_k) = k = n - 1 > 0$, where $(\cdot)^*$ denotes transpose and conjugate of a matrix, and Σ_k can be expressed as

$$\Sigma_k = \left(\begin{array}{ccc|c} \sigma_1 & & 0 & 0 \\ & \cdots & & \\ 0 & & \sigma_k & 0 \\ \hline & & 0 & 0 \end{array} \right), \quad (\sigma_1 \geq \sigma_2 \geq \cdots \sigma_k \geq 0)$$

then we get the following results

1. Out of all matrices of rank k , the matrix A_k is the one which closest to A .
2. The distance from A to A_k : $\|A - A_k\|_2 = \sigma_n$.
3. The perturbation $A - A_k = \sigma_n v_n u_n^*$

Therefore, the distance σ_n and perturbation $\sigma_n v_n u_n^*$ are then obtained. If the smallest nonzero singular value σ_n is very small, implying that the matrix is very close to a matrix of rank $n - 1$.



3.3.3 An Algorithm to Compute the Distance

There are many methods to solve $\sigma_{\min}[\mathbf{A} - s\mathbf{I}, \mathbf{B}]$, such as Newton's methods introduced by L. Elsner and C.He [11], or an iterative algorithm proposed by Mark Wicks and R. A. DeCarlo [7] and others (e.g., [3], [24], [26]). In the section, we introduce the method proposed by Mark Wicks and R. A. DeCarlo [7].

Although the formula of (3.13) is the most attractive formulation of $\mu(\mathbf{A}, \mathbf{B})$, DeCarlo gave a new interpretation, which is based on the observation that the pair (\mathbf{A}, \mathbf{B}) is uncontrollable, then there exists a partitioning and a equivalent transformation for which the pair:

$$\hat{\mathbf{A}} = \begin{pmatrix} A_{11} & A_{12} \\ A_{21} & A_{22} \end{pmatrix}, \quad \hat{\mathbf{B}} = \begin{pmatrix} B_1 \\ B_2 \end{pmatrix} \quad (3.18)$$

has the submatrices A_{21} and B_2 equal to zero. To compute the distance form pair (\mathbf{A}, \mathbf{B})

to lower rank, only the perturbations having a rank of one or two are interest, which implies that A_{11} has dimension $(n-1) \times (n-1)$ or $(n-2) \times (n-2)$. Using this approach, $\mu(\mathbf{A}, \mathbf{B})$ becomes the minimum of $\| [A_{21} \ B_2] \|$ over all unitary bases for the state space, the minimization is

$$\mu(\mathbf{A}, \mathbf{B}) = \min_{q \in \mathbb{C}^n} \| [q^* \mathbf{A} (I - qq^*) q^* \mathbf{B}] \| \quad (3.19)$$

subject to $q^* q = 1$. Here, we leave out the procedure of proof and only illustrate an algorithm since it is very complex. Define the distance measure

$$\begin{aligned} d(\mathbf{A}, \mathbf{B}) &= \| [e_n^* (A(I - e_n e_n^*) B)] \| \\ &= \sum_{j=1}^{n-1} |a_{nj}|^2 + \sum_{j=1}^m |b_{nj}|^2 \end{aligned} \quad (3.20)$$

where e_n denotes the n -th standard basis vector for \mathbb{R}^n . Following, we give the algorithm to compute the distance.

Algorithm 3.1 The Algorithm to Compute $d(\mathbf{A}, \mathbf{B})$

- (1) Set $A_1 = \mathbf{A}$, $B_1 = \mathbf{B}$.
- (2) Let $M_k = [A_k - [a_{nn}]_k I \ B_k]$.
- (3) Factor M_k as the product of a lower triangular matrix L_k and a unitary matrix U_k where $M_k = L_k U_k$.
- (4) Factor L_k as the product of a unitary matrix Q_k and a right upper triangular matrix R_k , i.e., $L_k = Q_k R_k$.
- (5) Set $A_{k+1} = Q_k^* A_k Q_k$, $B_{k+1} = Q_k^* B_k$
- (6) If $|d(A_{k+1}, B_{k+1}) - d(A_K, B_k)| \leq \text{tol}$, then stop; otherwise set $k = k + 1$, and go back to (2).

where tol is the tolerance to be defined.

About detailed interpretations of this algorithm, see reference [7].

3.3.4 Spacecraft Example

Now, we lead spacecraft linear model (3.6)-(3.7) into Algorithm 3.1 and obtain the distance to nearest uncontrollable set of each faulty case and the corresponding location

Table 3.2: Distance to uncontrollable

Condition	B	B_1	B_2	B_3	B_4
Distance	0.56	0.3775	0.3775	0.3775	0.3775
S_*	2.53×10^{-20}	2.01×10^{-6}	2.01×10^{-6}	-2.01×10^{-6}	-2.01×10^{-6}
Condition	B_{12}	B_{13}	B_{14}		
Distance	1.02×10^{-6}	7.88×10^{-7}	1.22×10^{-6}		
S_*	3.75×10^{-10}	1.15×10^{-29}	4.97×10^{-6}		
Condition	B_{23}	B_{24}	B_{34}		
Distance	1.22×10^{-6}	7.88×10^{-7}	1.02×10^{-6}		
S_*	4.97×10^{-6}	1.15×10^{-29}	-3.75×10^{-10}		

of s , denoted by S_* , where are listed in Table 3.2.

It is obviously that the distance of the cases of two actuators fail are at least 10^{-5} to 10^{-6} times shorter than those of normal or one actuators fail. Comparing Table 3.2 to Table 3.1, we can see that the cases which need more energy to transfer states when two actuator fail in Table 3.1 are corresponding to the ones of shorter distance to uncontrollable in Table 3.2. Rather than discussing a special situation (i.e., to transfer state from $x(0) = (-0.7, -0.07, 1.5, 0.3, 1.3, -0.2)^T$ to $\mathbf{0}$), we give a more general concept to uncontrollable measure. Finally, we list the perturbations of two cases, say $B_f = B$ and $B_f = B_{12}$.

when $B_f = B$,

$$\delta A = \begin{pmatrix} -4.74 \times 10^{-26} & -2.83 \times 10^{-8} & 0 & 0 & 2.56 \times 10^{-10} & -6.07 \times 10^{-25} \\ -7.01 \times 10^{-38} & -4.18 \times 10^{-20} & 0 & 0 & 3.78 \times 10^{-22} & 8.97 \times 10^{-37} \\ 0 & 0 & 0 & 0 & 0 & 0 \\ 0 & 0 & 0 & 0 & 0 & 0 \\ 7.64 \times 10^{-42} & 4.56 \times 10^{-24} & 0 & 0 & -4.12 \times 10^{-26} & -9.78 \times 10^{-41} \\ -1.58 \times 10^{-22} & -9.42 \times 10^{-5} & 0 & 0 & 8.51 \times 10^{-7} & 2.02 \times 10^{-21} \end{pmatrix}$$

$$\delta B = \begin{pmatrix} -8.41 \times 10^{-5} & -8.41 \times 10^{-5} & 8.41 \times 10^5 & 8.41 \times 10^{-5} \\ -1.24 \times 10^{-16} & -1.24 \times 10^{-16} & 1.24 \times 10^{-16} & 1.24 \times 10^{-16} \\ 0 & 0 & 0 & 0 \\ 0 & 0 & 0 & 0 \\ -1.36 \times 10^{-20} & 1.36 \times 10^{-20} & -1.36 \times 10^{-20} & -1.36 \times 10^{-20} \\ -0.28 & -0.28 & 0.28 & 0.28 \end{pmatrix}$$

when $B_f = B_{12}$,

$$\delta A = \begin{pmatrix} -1.25 \times 10^{-10} & -8.46 \times 10^{-20} & 1.26 \times 10^{-37} & -3.36 \times 10^{-28} & 1.49 \times 10^{-10} \\ -2.53 \times 10^{-7} & -1.72 \times 10^{-16} & 2.55 \times 10^{-34} & -6.8 \times 10^{-25} & 3.03 \times 10^{-7} \\ 1.55 \times 10^{-25} & 1.05 \times 10^{-34} & 1.56 \times 10^{-52} & -4.16 \times 10^{-43} & -1.85 \times 10^{-25} \\ -4.65 \times 10^{-24} & -3.15 \times 10^{-33} & 4.68 \times 10^{-51} & -1.25 \times 10^{-41} & 5.56 \times 10^{-24} \\ 5.22 \times 10^{-11} & -3.24 \times 10^{-20} & 5.25 \times 10^{-38} & 1.4 \times 10^{-28} & -6.24 \times 10^{-11} \\ -6.05 \times 10^{-7} & -4.1 \times 10^{-16} & 6.09 \times 10^{-34} & -1.63 \times 10^{-24} & 7.24 \times 10^{-7} \end{pmatrix}_{\text{column1-5}}$$

$$\begin{pmatrix} 7.18 \times 10^{-20} \\ 1.45 \times 10^{-16} \\ -8.9 \times 10^{-35} \\ 2.67 \times 10^{-33} \\ -3 \times 10^{-20} \\ 3.48 \times 10^{-16} \end{pmatrix}_{\text{column6}}$$

$$\delta B = \begin{pmatrix} 0 & 0 & 1.01 \times 10^{-16} & 1.01 \times 10^{-16} \\ 0 & 0 & 2.05 \times 10^{-13} & 2.05 \times 10^{-13} \\ 0 & 0 & -1.25 \times 10^{-31} & -1.25 \times 10^{-31} \\ 0 & 0 & 3.77 \times 10^{-30} & 3.77 \times 10^{-30} \\ 0 & 0 & -4.23 \times 10^{-17} & -4.23 \times 10^{-17} \\ 0 & 0 & 4.91 \times 10^{-13} & 4.91 \times 10^{-13} \end{pmatrix}$$

Since the distances of system (\mathbf{A}, \mathbf{B}) to uncontrollable for the cases of two actuators fail are much smaller than those of normal or one actuator fail, the perturbation $\mathbf{A} - \mathbf{A}_k$ of faulty condition B_{12} is much smaller than faulty condition B . In order to see the quantity of perturbations, we define a quantitative measure

$$Q = \sum |\delta A| + \sum |\delta B| \quad (3.21)$$

After calculation, we can get $Q_B = 1.1204$ and $Q_{B_{12}} = 1.89 \times 10^{-6}$, which implies that the faulty system B_{12} will become uncontrollable only affected by a very small perturbation, while the faulty one B will not.

3.4 Mobility of Eigenvalues

3.4.1 Introduction

The controllability measure suggested in section 3.3 is related to the distance from a controllable system to a nearest uncontrollable one, the measure requires minimizing the singular value of a polynomial matrix which can be computationally involved. In the section, we introduce another controllability measure proposed by M. Tarakh [31],

[33], [34], which is a new concept named "Mobility of Eigenvalues", and we will discuss a system with distinct and repeated eigenvalues, respectively. About the case of distinct eigenvalue, we will start from two different viewpoints of mobility such that will lead to the same result, which will be discussed in part I and part II, respectively.

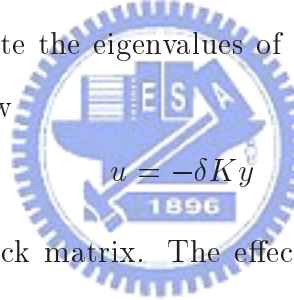
3.4.2 System with Distinct Eigenvalues (Part I)

Consider a linear multivariable system

$$\dot{x} = \mathbf{A}x + \mathbf{B}u \quad (3.22)$$

$$y = \mathbf{C}x \quad (3.23)$$

where $x \in \mathbb{R}^n$, $u \in \mathbb{R}^m$ and $y \in \mathbb{R}^l$ are state, input and output vectors, respectively, and \mathbf{A} , \mathbf{B} , and \mathbf{C} are matrices with appropriate dimensions. The mobility of an eigenvalue of the system (3.22)-(3.23) can be defined as the ratio of the neighborhood to which it may be shifted to the control gain used to cause such a change. More precisely, consider the system (3.22)-(3.23), and denote the eigenvalues of \mathbf{A} as λ_i , $i = 1, 2, \dots, n$. Now apply the output feedback control law

$$u = -\delta K y \quad (3.24)$$


where δK is the $m \times l$ feedback matrix. The effect of the feedback control will bring the eigenvalues λ_i of the open loop system ($\mathbf{A}, \mathbf{B}, \mathbf{C}$) to $\hat{\lambda}_i = \lambda_i + \delta \lambda_i$, where $\hat{\lambda}_i$ is the eigenvalue of the closed loop system matrix ($\mathbf{A} - \mathbf{B}\delta K\mathbf{C}$). Then we define the *mobility* of the eigenvalue λ_i under such output feedback as

$$\mu_i = \left\| \frac{\delta \lambda_i}{\delta K} \right\|_F \quad (3.25)$$

where

$$\frac{\delta \lambda_i}{\delta K} = \begin{pmatrix} \frac{\delta \lambda_i}{\delta K_{11}} & \cdots & \frac{\delta \lambda_i}{\delta K_{1l}} \\ \vdots & & \vdots \\ \frac{\delta \lambda_i}{\delta K_{m1}} & \cdots & \frac{\delta \lambda_i}{\delta K_{ml}} \end{pmatrix} \quad (3.26)$$

and $\|\cdot\|_F$ is the Frobinus norm.

Suppose e_i and f_i are the right and left eigenvectors of \mathbf{A} with associated eigenvalue, respectively, that is, $\mathbf{A}e_i = \lambda_i e_i$, $f_i^* \mathbf{A} = \lambda_i f_i^*$, for $i = 1, 2, \dots, n$. Note that the pair $(f_i^*$,

e_j), $i \neq j$ are biorthogonal (i.e., $f_i^* e_j = 0$), and we can always achieve both $f_i^* e_i = 1$ and $e_i^* e_i = 1$, in which case $f_i^* f_i \neq 1$, in general. It is shown (see Appendix 3A) that the eigenvalue $\hat{\lambda}_i$ of the matrix $(\mathbf{A} + \delta D)$, where δD is an $n \times n$ perturbation matrix whose elements are sufficient small, can be expressed as

$$\hat{\lambda}_i = \lambda_i + \delta \lambda_i \quad (3.27)$$

and $\delta \lambda_i$ can be obtained from

$$\delta \lambda_i = \frac{f_i^* \delta D e_i}{f_i^* e_i} \quad (3.28)$$

In the meanwhile, we should utilize Remark 3.1 below.

Remark 3.1 Assume K is a $m \times n$ matrix whose elements are α_{ab} , $a = 1, 2, \dots, m$ and $b = 1, 2, \dots, n$. Define $u = (u_1 \ u_2 \ \dots \ u_m)^T$ and $v = (v_1 \ v_2 \ \dots \ v_n)^T$ are two vectors, let a function f be $f = u^T K v$, then we can express $\frac{\partial f}{\partial K}$ as

$$\frac{\partial f}{\partial K} = \begin{pmatrix} \frac{\partial f}{\partial \alpha_{11}} & \cdots & \frac{\partial f}{\partial \alpha_{1n}} \\ \vdots & \ddots & \vdots \\ \frac{\partial f}{\partial \alpha_{m1}} & \cdots & \frac{\partial f}{\partial \alpha_{mn}} \end{pmatrix} = \begin{pmatrix} u_1 v_1 & \cdots & u_1 v_n \\ \vdots & \ddots & \vdots \\ u_m v_1 & \cdots & u_m v_n \end{pmatrix} = u v^T \quad (3.29)$$

Using this result and $f_i^* e_i = 1$ and the fact that in the closed loop system, $\delta D \equiv \mathbf{B} \delta K \mathbf{C}$, we can get

$$\delta \lambda_i = f_i^* \delta D e_i = (f_i^* \mathbf{B}) \delta K (\mathbf{C} e_i) \quad (3.30)$$

then adopt equation (3.29)

$$\frac{\delta \lambda_i}{\delta K} = (f_i^* \mathbf{B})^* (\mathbf{C} e_i)^* \quad (3.31)$$

thus we can have

$$\mu_i = \left\| \frac{\delta \lambda_i}{\delta K} \right\|_F = \left\| \mathbf{C} e_i f_i^* \mathbf{B} \right\|_F \quad (3.32)$$

Following, we will show that μ_i is equal to another controllability measure m_i in part II.

3.4.3 System with Distinct Eigenvalues (Part II)

The input-output transfer function of the system (3.22)-(3.23) is

$$Y(s) = \mathbf{C}(sI - \mathbf{A})^{-1} \mathbf{B} u(s) = \frac{\phi(s)}{\Delta(s)} u(s) \quad (3.33)$$

where $\phi(s) = \mathbf{C} \operatorname{adj}(sI - \mathbf{A})\mathbf{B}$ is the $l \times m$ numerator transfer function matrix, and $\Delta(s)$ is the characteristic polynomial. In order to discuss controllability, we can set $\mathbf{C} = I_n$, then define a new numerator matrix $\phi_M(s)$ as

$$\phi_M(s) = \operatorname{adj}(sI - \mathbf{A})\mathbf{B} \quad (3.34)$$

then we propose the following result.

Proposition 3.1 [27], [32] Consider a system $(\mathbf{A}, \mathbf{B}, \mathbf{C})$ and the eigenvalues λ_i , $i = 1, 2, \dots, n$ of \mathbf{A} are distinct. The mode λ_i is uncontrollable if and only if $\phi_M(\lambda_i) = 0$.

Proof: This proposition is based on the fact that if a system is with distinct eigenvalues, common pole-zero cancellations between all the entries of the transfer function matrix $\mathbf{C}(sI - \mathbf{A})^{-1}\mathbf{B}$ result in uncontrollability or unobservability. Previously, we had let $\mathbf{C} = I_n$, it is obviously that the system (3.22)-(3.23) must be observable, implying that it must be uncontrollable while pole-zero cancellations occur. Since when mode λ_i is uncontrollable, pole-zero cancellations happened between all the elements of the matrix $(sI - \mathbf{A})^{-1}\mathbf{B}$, it means that all the items of $\phi_M(s)$ have the factor $(s - \lambda_i)$, which make $\phi_M(\lambda_i) = 0$. ■

Following, we define the controllability measurement.

Definition 3.2 Consider a system $(\mathbf{A}, \mathbf{B}, \mathbf{C})$ and the eigenvalues of \mathbf{A} are distinct. The controllability measure m_i of the mode λ_i is defined

$$m_i = \|\phi_M(\lambda_i)\|_F \quad (3.35)$$

where $\phi_M(\lambda_i)$ is the $n \times m$ numerator matrix as defined in equation (3.34) with s is replaced by λ_i . ■

In addition to determine the controllability of particular mode λ_i , we can define

$$m_o = \min_i \{m_i\} \quad (3.36)$$

which is a controllability measure for the overall system $(\mathbf{A}, \mathbf{B}, \mathbf{C})$. Following, we will deal with equation(3.35).

Suppose e_i and f_i are the right and left eigenvectors of \mathbf{A} as defined in part I, define $E = (e_1 \ e_2 \ \cdots \ e_n)$ and $F = (f_1 \ f_2 \ \cdots \ f_n)$, it is obviously that $EF^* = FE^* = I_n$. Since \mathbf{A} has distinct eigenvalue, then \mathbf{A} can be expressed as $\mathbf{A} = E\Lambda F^*$, where $\Lambda = \text{diag}\{\lambda_i\}$. In the view of these, equation (3.34) with s is replaced by λ_i can be

$$\begin{aligned}\phi_M(\lambda_i) &= \text{adj}(\lambda_i I - E\Lambda F^*)\mathbf{B} \\ &= \text{adj}(E(\lambda_i I - \Lambda)F^*)\mathbf{B} \\ &= \text{adj}(F^*) \text{adj}(\lambda_i I - \Lambda) \text{adj}(E) \mathbf{B}\end{aligned}\quad (3.37)$$

Since $EF^* = I$ and $|E||F^*| = |EF^*| = |I| = 1$, we can get $E = (F^*)^{-1} = \text{adj}(F^*)/|F^*|$ or equivalently, $\text{adj}(F^*) = |F^*|E$, and we can get $\text{adj}(E) = |E|F^*$ in the same manner. Therefore, equation (3.37) can be rewritten as

$$\phi_M(\lambda_i) = E \text{adj}(\lambda_i I - \Lambda)F^*\mathbf{B}\quad (3.38)$$

now, $\text{adj}(\lambda_i I - \Lambda)$

$$= \text{adj} \begin{pmatrix} \lambda_i - \lambda_1 & & & & \\ & \ddots & & & \\ & & \lambda_i - \lambda_i & & \\ & & & \ddots & \\ & \mathbf{0} & & & \lambda_i - \lambda_n \end{pmatrix} = \begin{pmatrix} 0 & & & & \\ & \ddots & & & \\ & & \delta_i & & \mathbf{0} \\ & & & \ddots & \\ \mathbf{0} & & & & 0 \end{pmatrix}\quad (3.39)$$

where

$$\delta_i = \prod_{j=1, j \neq i}^n (\lambda_i - \lambda_j) \quad j \neq i\quad (3.40)$$

is a constant scalar and is located on the i -th position of the i -th column vector. Substituting $\text{adj}(\lambda_i I - \Lambda)$ in the express of equation (3.38) for $\phi_M(\lambda_i)$, we obtain

$$\phi_M(\lambda_i) = \delta_i e_i f_i^* \mathbf{B}\quad (3.41)$$

then the controllability measure can now be expressed as

$$m_i = \|\phi_M(\lambda_i)\|_F = |\delta_i| \|e_i f_i^* \mathbf{B}\|_F\quad (3.42)$$

Now, we can see the relation between μ_i (3.32) and m_i (3.42), setting $\mathbf{C} = I_n$ in equation (3.32) result in

$$\mu_i = \left\| \frac{\delta \lambda_i}{\delta K} \right\|_F = \|e_i f_i^* \mathbf{B}\|_F \quad (3.43)$$

then m_i is $|\delta_i|$ times of μ_i , where $|\delta_i|$ is a constant when the system is given. Therefore, we claim that μ_i and m_i are the same, and the controllability measure m_i in part II is also the mobility.

Let's go on from equation (3.42). Since $\text{adj}(\lambda_i I - \Lambda)$ having a rank of one, and $\phi_M(\lambda_i)$ is never a null matrix (otherwise the system is uncontrollable), it is obviously that $\phi_M(\lambda_i)$ is of unity rank. Note also that as long as $\phi_M(\lambda_i)$ have only one nonzero singular value, which implying that $\phi_M^*(\lambda_i)\phi_M(\lambda_i)$ also have only one nonzero eigenvalue, hence $\lambda_{max}[\phi_M^*(\lambda_i)\phi_M(\lambda_i)] = \text{tr}[\phi_M^*(\lambda_i)\phi_M(\lambda_i)]$, where $\lambda_{max}[\cdot]$ and $\text{tr}[\cdot]$ denote maximum eigenvalue and the trace of the matrix. According to the definitions of the spectral norm and Frobinus norm, we can recognize they are equal in such instance, that is $\|\phi_M^*(\lambda_i)\|_S = \|\phi_M^*(\lambda_i)\|_F$, and either norm can be used, then the mobility is

$$\begin{aligned} m_i &= \|\phi_M(\lambda_i)\|_F = |\delta_i| [\text{tr}((e_i f_i^* \mathbf{B})^*(e_i f_i^* \mathbf{B}))]^{\frac{1}{2}} \\ &= |\delta_i| [\text{tr}(\mathbf{B}^T f_i \cdot e_i^* e_i f_i^* \mathbf{B})]^{\frac{1}{2}} \\ &= |\delta_i| [\text{tr}(e_i^* e_i f_i^* \mathbf{B} \mathbf{B}^T f_i)]^{\frac{1}{2}} \end{aligned} \quad (3.44)$$

using previous definition that $e_i^* e_i = 1$ we can obtain the final result

$$m_i = |\delta_i| [f_i^* \mathbf{B} \mathbf{B}^T f_i]^{\frac{1}{2}} \quad (3.45)$$

where the quadratic form $f_i^* \mathbf{B} \mathbf{B}^T f_i = \|\mathbf{B}^T f_i\|_F^2$ which is real and positive semidefinite, and $|\delta_i|$ is never zero due to the fact that the eigenvalues are distinct. Therefore, we can obtain the result below.

Lemma 3.1 For a system pair (\mathbf{A}, \mathbf{B}) , if the system eigenvalue λ_i and the corresponding left eigenvector f_i are all real, then the mobility m_i of λ_i is

$$m_i = |\delta_i| [f_i^T \mathbf{B} \mathbf{B}^T f_i]^{\frac{1}{2}} \quad (3.46)$$

the mobility m_i becomes zero only when f_i is orthogonal to all the rows of \mathbf{B}^T , or equivalently, all the columns of \mathbf{B} . ■

Lemma 3.2 For a system pair (\mathbf{A}, \mathbf{B}) , the pair of complex conjugate eigenvalues $\lambda_i = \lambda_{i1} + j\lambda_{i2}$ and $\lambda_i^* = \lambda_{i1} - j\lambda_{i2}$ with associated eigenvectors $f_i = f_{i1} + jf_{i2}$ and $f_i^* = f_{i1}^T - jf_{i2}^T$, the mobility m_i becomes

$$m_i = |\delta_i| [f_{i1}^T \mathbf{B} \mathbf{B}^T f_{i1} + f_{i2}^T \mathbf{B} \mathbf{B}^T f_{i2}]^{\frac{1}{2}} \quad (3.47)$$

the eigenvalue pair (λ_i, λ_i^*) is uncontrollable if and only if both f_{i1} and f_{i2} are orthogonal to all the rows of \mathbf{B}^T . ■

3.4.4 System with Repeated Eigenvalues

The analysis of last section is based on Proposition 3.1 which gives conditions on zeros of the elements of the numerator matrix $\phi(s)$ for mobility of the system with distinct eigenvalues. In fact, these elements are the zero polynomials of the SISO subsystems. It has been proved that for determining the controllability of the system having repeated eigenvalues, one must consider not only the zeros of the SISO subsystems, but also the zeros of other square subsystems. This is due to the fact that a system can have $\phi_M(\lambda_i) = 0$ and still controllable when eigenvalues are repeated [29]. Now, we utilize the transmission zeros to define mobility for a general system with repeated eigenvalues.

Consider the set of r -input r -output (r -dimensional) square subsystem of the system $(\mathbf{A}, \mathbf{B}, \mathbf{C})$, $r = 1, 2, \dots, \min(m, l)$ which denoted by $(\mathbf{A}, \mathbf{B}_\alpha^r, \mathbf{C}_\beta^r)$, and \mathbf{B}_α^r , $\alpha = 1, 2, \dots, u_r$, are the set of $n \times r$ submatrices formed by r columns of the matrix \mathbf{B} , and \mathbf{C}_β^r , $\beta = 1, 2, \dots, v_r$, are the set of $r \times n$ submatrices formed by r rows of the matrix \mathbf{C} . The number of the $n \times r$ submatrices of \mathbf{B} is $u_r = (m! / (m-r)! r!)$ and the number of the $r \times n$ submatrices of \mathbf{C} is $v_r = (l! / (l-r)! r!)$. Besides, the number of r -dimensional subsystem is $w_r = u_r v_r$, and the total number of subsystems is $w = \sum_{r=1}^{\min(m, l)} w_r$, and the transfer function matrix of the subsystem is $G_\gamma^r(s) = \mathbf{C}_\beta^r (sI - A)^{-1} \mathbf{B}_\alpha^r$, $\gamma = 1, 2, \dots, w_r$.

Base on the definition of the zero polynomial of a system [14], we can express the set of zero polynomials of the r -dimensional subsystems as

$$\begin{aligned} z_\gamma^r(s) &= \det \begin{bmatrix} sI - A & \mathbf{B}_\alpha^r \\ \mathbf{C}_\beta^r & 0 \end{bmatrix} \\ &= |sI - A| |\mathbf{C}_\beta^r (sI - A)^{-1} \mathbf{B}_\alpha^r| \\ &= |\mathbf{C}_\beta^r \text{adj}(sI - A) \mathbf{B}_\alpha^r| \end{aligned} \quad (3.48)$$

where the roots of $z_\gamma^r(s)$ are the transmission zeros of the r -dimensional subsystems. Furthermore, the zero polynomials of one dimensional subsystems are the entries of the numerator transfer function matrix $\phi(s)$.

According, [31], if the control law to be applied to the system (3.22)-(3.23) is

$$u = -Ky \quad (3.49)$$

where K is constant $m \times l$ feedback matrix, the closed loop characteristic polynomial of system (3.22)-(3.23) with such a control law is

$$\hat{\Delta}(s) = \Delta(s) + \sum_{r=1}^{\min(m,l)} \sum_{\gamma=1}^{w_r} \det(K_\gamma^r) z_\gamma^r(s) \quad (3.50)$$

where $\Delta(s)$ is the open loop characteristic polynomial of the system, K_γ^r is the $r \times r$ submatrices obtained from the $l \times m$ matrix K^T at the same manner as the subsystem $G_\gamma^r(s)$ is obtained from the system $G(s)$, and those will be used to establish the following result.

Proposition 3.2 The mode λ_i is uncontrollable if and only if all the r -dimensional subsystems of $(\mathbf{A}, \mathbf{B}, I_n)$ have a transmission zero at λ_i , that is, $z_\gamma^r(s) = 0$ for all r and γ .

Proof: The proof is directly from equation (3.50) by setting $\mathbf{C} = I_n$, and the system is controllable if and only if all the roots of its closed loop characteristic polynomial $\hat{\Delta}(s)$ are affected by an arbitrary feedback. In this case, only if λ_i is not a transmission zero of all subsystems, in other words, $z_\gamma^r(\lambda_i) \neq 0$ for some r and γ , as seen from equation (3.50). Based on above developments, the mobility of the mode λ_i of a system with repeated eigenvalues is defined as

$$m_i = \left[\sum_{r=1}^{\min(m,l)} \sum_{\gamma=1}^{w_r} |z_\gamma^r(\lambda_i)|^2 \right]^{\frac{1}{2}} \quad (3.51)$$

where $z_\gamma^r(\lambda_i)$ is obtained after replacing \mathbf{C}_β^r by I_β^r and I_β^r are appropriate $r \times n$ submatrices of I_n . ■

3.4.5 Mobility of Spacecraft

Here, we determine the mobility of the spacecraft linear model (3.6)-(3.7). It is known that the characteristic polynomial of the spacecraft system is $\lambda^2 \cdot [\lambda^4 + (a_1 + a_2^2)\lambda^2 - 2a_1^2] =$

0, and the six eigenvalues are $(0, 0, \pm\mu_1, \pm j\mu_2)$, where $\mu_1 = \sqrt{\frac{\sqrt{(a_1+a_2)^2+8a_1^2}-(a_1+a_2)}{2}}$ and $\mu_2 = \sqrt{\frac{\sqrt{(a_1+a_2)^2+8a_1^2}+(a_1+a_2)}{2}}$. Clearly, that the spacecraft system is of the case of repeated eigenvalues. Since the mobility measure of repeated eigenvalues system which discussed last subsection are complicated, Tarokh proposed an alternative method to determine the mobility. He suggested that we can apply small perturbations to the original system and obtain a system with distinct eigenvalues. According to the setting of the spacecraft model we defined before, the minimum value of the entries of \mathbf{A} is about 10^{-7} , for this reason, we define a small perturbation $\epsilon = 10^{-10}$, which is 1000 times smaller. Then we add ϵ to position (3,3) of matrix \mathbf{A} in equations (3.6)-(3.7), the characteristic polynomial becomes

$$\lambda(\lambda - \epsilon)[\lambda^4 + (a_1 + a_2^2)\lambda^2 - 2a_1^2] = 0 \quad (3.52)$$

which implies that one of the eigenvalue 0 has been moved to location ϵ , and the six eigenvalues become $(0, \epsilon, \pm\mu_1, \pm j\mu_2)$. Since the difference between μ_i and m_i is δ_i which is a constant while a system is given, we eliminate δ_i utilize the over all system mobility as

$$m_o = \min_i \{m_i\} = \min_i \{[f_i^* \mathbf{B} \mathbf{B}^T f_i]^{\frac{1}{2}}\} \quad (3.53)$$

After calculating, we get the mobility of each cases as listed in the table below

Table 3.3: Mobility of spacecraft system

Condition	B	B_1	B_2	B_3	B_4
Mobility	310.09	268.54	268.54	268.54	268.54
Condition	B_{12}	B_{13}	B_{14}		
Mobility	219.27	219.27	219.27		
Condition	B_{23}	B_{24}	B_{34}		
Mobility	219.27	219.27	219.27		

From Table 3.3, we can see that the mobility is decreased when less healthy actuators remainder, indicating that the system is less controllable, too.

Appendix 3A

Suppose $A \in \mathbb{R}^{n \times n}$ and let x and y be, respectively, the right and left eigenvectors associated with a simple eigenvalue λ of A , that is, $Ax = \lambda x$ and $y^* A = \lambda y^*$, we will show that if E is a small perturbation matrix, then

$$\lambda + \frac{y^* E x}{y^* x} \tag{3A.1}$$

is an eigenvalue of $A + E$.

proof

First, we define α_{ij} be the ij -th element of E , and $E_{ij} = e_i e_j^T$ for $i, j = 1, 2, \dots, n$, where e_i and e_j are corresponding vectors of standard basis for \mathbb{R}^n . Rewrite λ as

$$\lambda = \frac{y^* A x}{y^* x} \tag{3A.2}$$

now, if we apply a small perturbation $tE_{i,j}$ in the ij -th direction of A , we will have

$$(A + tE_{i,j})x(t) = \lambda(t)x(t) \tag{3A.3}$$

where $\lambda(t)$ and $x(t)$ denote the eigenvalue and associated eigenvector of A while affected by the perturbation. By the same manner as equation (3A.2), we can expressed $\lambda(t)$ as

$$\lambda(t) = \frac{y^*(A + tE_{i,j})x(t)}{y^*x(t)} \tag{3A.4}$$

note that the expression of λ can have another form

$$\lambda = \frac{y^* A x(t)}{y^* x(t)} \tag{3A.5}$$

then the variation of λ in the ij -th direction is

$$\begin{aligned} \frac{\partial \lambda}{\partial \alpha_{ij}} &= \lim_{t \rightarrow 0} \frac{\lambda(t) - \lambda}{t} \\ &= \lim_{t \rightarrow 0} \frac{y^*(A + tE_{i,j})x(t) - y^* A x(t)}{t y^* x(t)} \\ &= \lim_{t \rightarrow 0} \frac{y^* E_{i,j} x(t)}{y^* x(t)} \\ &= \lim_{t \rightarrow 0} \frac{y^* E_{i,j} x}{y^* x} \end{aligned} \tag{3A.6}$$

It is obviously that if the variation of λ in the i, j -th direction of A has the form as shown in equation (3A.6), we can know that the small change $\delta\lambda$ of λ due to the perturbation E must be

$$\delta\lambda = \frac{y^* E x}{y^* x} \quad (3A.7)$$

that is , $\lambda + \delta\lambda$ is an eigenvalue of $A + E$, where $\delta\lambda$ as stated above.



CHAPTER FOUR

CONCLUSIONS AND SUGGESTIONS FOR FURTHER RESEARCH

In this thesis, we study the spacecraft attitude tracking problem and new controllability measurements.

As is well known, the conventional Variable Structure Control (VSC) design suffers from chattering effect when using a sign-type controller and only achieves uniformly ultimate boundedness while using a saturation-type one. Therefore, we proposed a modified VSC scheme to improve these drawbacks. This modified VSC law behaves similarly to the sign-type and saturation-type VSC laws when the system state is far from and close to the selected sliding surface, respectively, and is continuous everywhere. As a result, this control law can eliminate the chattering phenomenon and achieve asymptotic stability. Consequently, the modified VSC scheme not only inherits from conventional VSC design the advantages of fast response and small sensitivity to model uncertainties and disturbances, but also enables a spacecraft to perform a highly accurate pointing task. Moreover, the proposed VSC scheme can be directly applied to existing sign or saturation-type VSC designs add to the applicability of our results. Simulation results have demonstrated the effectiveness of the proposed scheme. On the other hand, a class of reliable VSC laws are proposed and applied to spacecraft attitude control issue. These reliable VSC laws are shown to be able to tolerate the outage of actuators within a pre-specified subset of actuators in passive designs. While in active ones, the proposed fault detection and diagnosis mechanism is shown to be able to detect and diagnose the outage of the actuators, and provide a real-time information for reliable control. According to the simulations, it is shown that both passive and active reliable controllers can achieve the desired performance.

In chapter 3, we introduced two new concepts for controllability measurement, "Distance to Uncontrollable" ([3], [7], [10], [11], [24], [26]) and "Mobility of Eigenvalues" (Tarokh, [31], [33], [34]). Rather than giving absolute "yes" or "not" answers for controllability of classical measurement, the two methods guide the relative ideas into their measures, even can be connected with energy consumption of the system. Utilizing these benefits, we can analyze the system in a more clear and delicate way, instead of earning the information that whether a system is controllable or not, we can now get that how hard a system is to be controlled, which can tell us how much cost we should pay to achieve a specific task. Also, it provides helpful information while we design a system. The relation between the energy required to transfer the states and the degree of controllability of two methods are also presented in chapter 3. It shown that the more energy required, the more uncontrollable the system is, and vice versa.

To further extend the research covered in this thesis, we note several directions. In reliable control, to study and compare with other possible methods which can attenuate the chattering effect, and add more possible constraint in the design of VSC law due to the actuator physical limitation in mechanical system. For FDD design, to search a better way to estimate the faulty messages of actuators to avoid possible control high gain that might violate physical saturation restrictions. In controllability measurement, to study more subjects, compare their advantages and drawbacks, and their suitable applications. Further more, to extend those concepts to other control techniques, like switching control or fuzzy control, which are newly risen and attract more and more attention now.

References

- [1] G. Bajpai, B. C. Chang, and A. Lau, "Reconfiguration of flight control systems for actuators failures," *IEEE Aerospace and Electronic Systems Magazine*, vol. 16, no. 9, pp. 29-33, 2001.
- [2] B. R. Barmish, M. Corless, and G. Leitmann, "A new class of stabilizing controllers for uncertain dynamical Systems," *SIAM Journal of Control and Optimization*, vol. 21, no. 2, pp. 246-255, 1983.
- [3] D. L. Boley and W. S. Lu, "Measuring how far a controllable System is from an uncontrollable one," *IEEE Transactions on Automatic Control*, vol. AC-31, no. 3, pp. 249-251, 1986.
- [4] V. A. Chobotov, *Spacecraft Attitude Dynamics and Control*, Krieger Publishing Company, 1991.
- [5] C. T. Chen, *Linear System Theorey and Design*, 3rd edition, New York Oxford, 1999.
- [6] B. N. Datta, *Numerical Methods for Linear Control Systems*, Elsevier Inc, 2004.
- [7] M. Wicks and R. A. DeCarlo, "Computing the distance to an uncontrollable System," *IEEE Transactions on Automatic Control*, vol. 36, no. 1, pp.39-49, 1991.
- [8] C. Edwards and S. K. Spurgeon, "Sliding mode control: theory and appications," Taylor and Francis, 1998.
- [9] R. Eising, "The distance between a system and the set of uncontrollable systems" , *Proc. MTNS*, Beer-Sheva, Israel, June 1983, New York: Springer-Verlag, pp. 303-314, 1984.
- [10] R. Esing, "Between controllable and uncontrollable," *Systems and Control Letters*, vol. 4, pp. 263-264, July 1984.
- [11] L. Elsner and C. He, "An algorithm for computing the distance to uncontrollability," *Systems and Control Letters*, vol. 4, pp. 453-464, 1991.

- [12] J. Huang and C. F. Lin, "Numerical approach to computing nonlinear control laws," *Journal of Guidance, Control, and Dynamics*, vol. 18, no. 5, pp. 989-994, 1995.
- [13] J. Jiang and Q. Zhao, "Design of reliable control systems possessing actuator redundancies," *Journal of Guidance, Control, and Dynamics*, vol. 23, no. 4, pp. 706-710, 2000.
- [14] H. Kwakernaak and R. Sivan, *Linear optimal control*, Wiley-Interscience, New York, 1972.
- [15] F. Liao, J. L. Wang, and G. H. Yang, "Reliable robust flight tracking control: an LMI approach," *IEEE Transactions on Control Systems Technology*, vol. 10, no. 1, pp. 76-89, 2002.
- [16] Y. W. Liang, D. C. Liaw, and T. C. Lee, "Reliable control of nonlinear systems," *IEEE Transactions on Automatic Control*, vol. 45, no. 4, pp. 706-710, 2000.
- [17] Y. W. Liang, T. C. Chu, and C. C. Cheng, "Robust attitude control for spacecraft," *Proc. 2002 American Control Conference*, held at Anchorage, Alaska, USA, pp. 1342-1347, May 8-10, 2002.
- [18] Y. W. Liang, T. C. Chu, D. C. Liaw, and C.-C. Cheng, "Reliable control of nonlinear systems via variable structure scheme," *Proc. 2003 American Control Conference*, Denver, Colorado, USA, pp. 915-920, June 4-6, 2003.
- [19] Y. W. Liang, S. D. Xu, T. C. Chu, and C. C. Cheng, "Reliable output tracking control for a class of nonlinear systems," *IEICE Transactions on Fundamentals of Electronics, Communication, and Computer Sciences*, vol. E87-A, no. 9, pp. 2314-2321, 2004.
- [20] Y. W. Liang, S. D. Xu, T. C. Chu, C. C. Cheng, and D. C. Liaw, "Application of VSC reliable design to a spacecraft attitude tracking," *Proc. American Control Conference (ACC)*, Portland Oregon, USA, pp. 919-924, Jun. 8-10, 2005.

- [21] Y. W. Liang, S. D. Xu, T. C. Chu, C. L. Tsai, and C. C. Cheng, "VSC reliable design with application to a spacecraft attitude tracking," *IEEE International Conference on Industrial Technology (ICIT)*, Hong Kong, China, Dec. 14-17, 2005.
- [22] Y. W. Liang, S.-D. Xu, T. C. Chu, and C. L. Tsai, "Application of VSC reliable design to spacecraft attitude stabilization," *National Conference on Automatic Control*, Taiwan, R.O.C., Nov. 18-19, 2005.
- [23] Y. W. Liang, S.-D. Xu, and C. L. Tsai, "Study of VSC reliable designs with application to spacecraft attitude stabilization," *IEEE Transactions on Control Systems Technology*, 1st revised, 2006.
- [24] M. Gu, "New methods for estimating the distance to uncontrollability," *SIAM Journal on Matrix Analysis and Applications*, vol. 21, no. 3, pp. 989-1003, 2000.
- [25] D. D. Moerder, N. Halyo, J. R. Broussard, and A. K. Caglayan, "Application of precomputed control laws in a reconfigurable aircraft flight control system," *Journal of Guidance, Control, and Dynamics*, vol. 12, no. 3, pp. 325-333, 1989.
- [26] C. C. Paige, "Properties of numerical algorithms related to computing controllability," *IEEE Transactions on Automatic Control*, vol. AC-26, no. 1, pp.130-138, 1981.
- [27] C. R. Paul and Y. L. Kuo, "Controllability and observability of multivariable systems," *IEEE Transactions on Automatic Control*, vol. AC-16, pp. 207-209, 1971.
- [28] C. C. Teng, C. C. Chiou, and D. C. Liaw, "Design and analysis for the controller of ROCSAT-2 attitude control system," NSPO Technical Report, NSC-NSPO(A)-PC-FA06-01, 2001.
- [29] H. Seraji, "Transfer function matrix," *Electronic Letters*, vol. 23, no. 6, pp. 256-257, Mar. 1987.
- [30] J. J. E. Slotine and W. Li, *Applied nonlinear control*, Prentice-Hall, New Jersey, 1991.
- [31] M. Tarokh, "Fixed modes in multivariable systems using constrained controllers," *Automatica*, vol. 21, pp. 495-497, 1985.

- [32] M. Tarokh, "Frequency domain criteria for controllability and observability of multivariable systems," *Proc. American Control Conference*, Seattle, WA, 1986.
- [33] M. Tarokh, "Measures for controllability and eigenvalue mobility," *Proc. of the 29th Conference on Decision and Control*, Honolulu, Hawaii, pp. 1143-1148, Dec. 1990.
- [34] M. Tarokh, "Measures for controllability, observability and fixed," *IEEE Transactions on Automatic Control*, vol. 37, no. 8, pp.1268-1273, Aug. 1992.
- [35] V. I. Utkin, *Sliding Modes and Their Applications to Variable Structure Systems*, MIR Publishers, Moscow, Russia, 1978.
- [36] V. I. Utkin, "Variable structure systems with sliding modes," *IEEE Transactions on Automatic Control*, vol. 22, no. 2, pp. 212-222, 1997.
- [37] G. H. Yang, J. L. Wang, and Y. C. Soh, "Reliable guaranteed cost control for uncertain nonlinear systems," *IEEE Transactions on Automatic Control*, vol. 45, no. 11, pp. 2188-2192, 2000.

